5/20/24

Mechanistic Insights into Key Steps of Dinitrogen Reduction to Ammonia with Pincer-ligated Mo Complexes: Case Study of Easily Reduced PSP Mo Complexes

Santanu Malakar[‡], Souvik Mandal[‡], Xiaoguang Zhou[‡], Quinton Bruch, Rachel Allen, Laurence W. Giordano, Nicholas J. I. Walker, Thomas J. Emge, Faraj Hasanayn, Alexander J. M. Miller, Alan S. Goldman*

Abstract

The thioether-diphosphine pincer-ligated molybdenum complex, (PSP)MoCl₃ (1-Cl₃, PSP = 4,5bis(diisopropylphosphino)-2,7-di-tert-butyl-9,9-dimethyl-9H-thioxanthene) has been synthesized as a catalyst-precursor for N₂ reduction catalysis, with a focus on an integrated experimental/computational mechanistic investigation. The (PSP)Mo unit is isoelectronic with the (PNP)Mo (PNP = 2,6-bis(di-t-butylphosphinomethyl)pyridine) fragment found in the familyof catalysts for the reduction of N₂ to NH₃ first reported in 2011 by Nishibayashi and coworkers. Under an atmosphere of N₂ the reaction of **1-Cl₃** with three reducing equivalents yields the dinuclear penta-dinitrogen Mo complex $[(PSP)Mo(N_2)_2](\mu-N_2)$, **2**. Electrochemical studies reveal that 1-Cl₃ is significantly more easily reduced than (PNP)MoCl₃ (with a potential ca. 0.4 eV less negative). The bridging-nitrogen complex 2 shows no indication of undergoing N2 cleavage to Mo nitride complexes. The reaction of 1-Cl₃ with only two reducing equivalents, however, under N₂ atmosphere and in the presence of iodide, affords the product of N₂ cleavage, the nitride complex (PSP)Mo(N)(I). DFT calculations implicate another N2-bridged complex, $[(PSP)Mo(I)]_2(N_2)$, as a viable intermediate in facile N_2 cleavage to yield (PSP)Mo(N)(I). Conversion of the nitride ligand to NH₃ has been studied. If considering sequential addition of H atoms to the nitride, formation of the first N-H bond is by far the thermodynamically least favorable of the three N-H bond formation steps. The first N-H bond was formed by reaction of (PSP)Mo(N)(I) with [LutH]Cl, where coordination of Cl⁻ to Mo plays an essential role. Computations suggest that a second protonation, followed by a rapid and very favorable oneelectron reduction, and then a third protonation, furnishes ammonia. In agreement with calculations, ammonia can be generated using either mild H-atom transfer reagents or mild reductants/acids. This comprehensive analysis of the elementary steps of ammonia synthesis and the role of the central pincer donor and halide association provides guidance for future catalyst designs.

[‡]These co-authors contributed equally.

1. INTRODUCTION

The synthesis of ammonia from dinitrogen is perhaps the single most important industrially practiced chemical reaction, affording the fixed nitrogen for all synthetic fertilizer and thereby supporting approximately half of the world's food production.¹⁻² The current dominant process, based on fossil fuel reforming and Haber-Bosch catalysis is responsible for nearly 2% of the world's fossil fuel consumption and CO₂ emissions.¹⁻⁴ There is thus great interest in the development of electrochemically driven nitrogen reduction.⁵⁻¹⁷ Using a sustainable source of electrical energy, with water as the source of protons and electrons, such a process could in principle be essentially carbon-neutral. Such a process could also find applicability on a scale much larger even than the use of ammonia for fertilizer and chemicals, including the use of ammonia for storage and transportation of renewable energy or as a transportation fuel.^{4,15}

In 2003 Schrock reported that a (triamidoamine) Mo complex (Figure 1a) catalyzed the reduction and protonation of N₂ using Cp*₂Cr (Cp* = η^5 -C₅Me₅) as the source of electrons and Lutidine • H⁺ (LutH⁺) as the proton source. ¹⁸ This groundbreaking report represented the realization of a decades-old goal of a molecular catalyst for N₂ fixation; however, turnover numbers were quite low, selectivity for ammonia formation was low, and a very slow addition of reagents was required to achieve even these modest results. Nishibayashi subsequently reported ¹⁹⁻²⁰ that the pincer-ligated dimeric Mo complex $[(PNP)Mo(N_2)_2]_2(\mu-N_2)$ (PNP = 2,6bis(di-t-butylphosphinomethyl)pyridine) (Figure 1b) catalyzed a similar reaction more efficiently, and later that the corresponding trihalides and nitridohalides were equally or more effective as catalyst precursors. Since then Nishibayashi and others have reported numerous other examples of pincer-ligated Mo catalysts, some of which yield extremely high turnovers, including systems that can utilize water as the proton source.²¹⁻³⁴ Very recently, it was reported that addition of an electron-withdrawing substituent at the para-position of the pyridine ring (Figure 1b) dramatically enhanced catalytic activity with the use of SmI₂/H₂O as the source of electrons and protons.³⁴ In general, most of these catalysts have the "PYP pincer" motif in which two terminal dialkyl- or diarylphosphino groups are connected to a neutral coordinating group such as the pyridine group of PNP, a central phosphino group, or an N-heterocyclic carbene group. Other Mo-pincer complexes have also been found to effectively catalyze ammonia formation or, in some cases, to effect the key N2 cleavage step though not as part of an catalytic cycle for ammonia formation. 12,16,19-32,34-52

Figure 1. (a) Schrock's (triamidoamine)Mo catalyst. ^{18,53} (b) (PYP)Mo catalysts or catalyst precursors reported by Nishibayashi. ^{19,23,26,30} (c) (PSP)Mo complex reported in this work.

The examples illustrate great progress in the development of molecular catalysts for N₂ fixation, and in particular they indicate the promise of pincer-Mo complexes as catalysts for N₂ reduction/protonation. Such complexes have very recently been found to be active catalysts for electrochemical reduction of N₂ to NH₃ as well, with⁴⁵ or without⁵¹ a mediator. One of the challenges in the unmediated electrocatalysis is the need for highly negative applied potentials, which leads to competing H₂ evolution and presumably a high electrochemical overpotential; the development of a system with practical utility requires minimizing both of these factors¹¹. Thus we have been particularly interested in designing new pincer Mo catalysts that are easier to reduce, while still maintaining good catalytic activity. More broadly, we have sought to expand the chemical space of (PYP)Mo-based catalysts while attempting to learn about the reaction mechanisms and the factors that govern the energetics of the numerous steps in any cycle catalyzed by such species. In this context, we report here the development of a (PSP)Mo fragment (PSP = 4,5-bis(diisopropylphosphino)-2,7-di-tert-butyl-9,9-dimethyl-9H-thioxanthene) for N₂ reduction/protonation, the observation of several catalytically relevant intermediates and their reactions, and a computational study of this chemistry with comparison to Nishibayashi's archetypal (PNP)Mo catalysts.

2. EXPERIMENTAL RESULTS AND DISCUSSION

2.1. Synthesis and Characterization of (PSP)MoCl₃. PSP was synthesized as we have reported previously. State Its reaction with $MoCl_3(THF)_3$ in THF solution gave **1-Cl₃** (**1** = (PSP)Mo; Scheme 1). Crystals were obtained by diffusion of pentane into a THF solution, and the molecular structure was determined by single-crystal X-ray diffraction (scXRD) (Figure 2).

Scheme 1. Synthesis of (PSP)MoCl₃ (1-Cl₃)

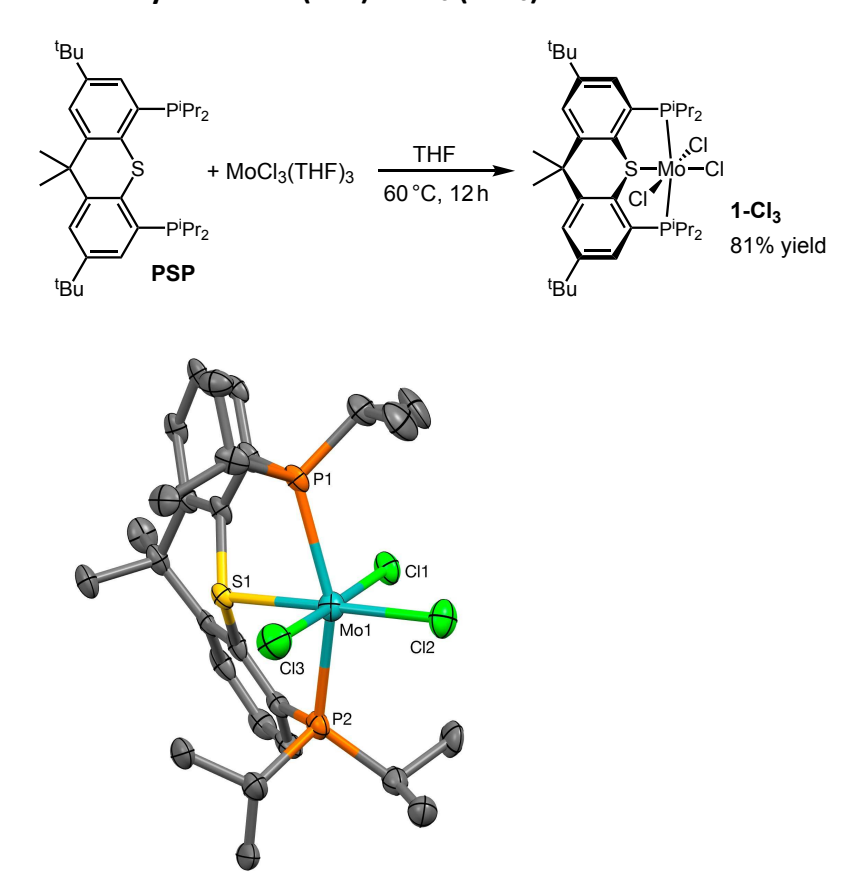


Figure 2. ORTEP representation (50% probability ellipsoids) of the structure of **1-Cl₃** determined by X-ray diffraction; hydrogen atoms and PSP t-butyl groups omitted for clarity. Selected bond lengths (Å) and angles (°): Mo1-S1, 2.473; Mo1-P1, 2.563; Mo1-Cl1, 2.435; Mo1-Cl2, 2.394; Mo1-Cl3, 2.358; S1-Mo1-P1, 76.99; S1-Mo1-P2, 76.04; P1-Mo1-P2, 152.81; S1-Mo1-Cl1, 84.18, Cl1-Mo1-Cl2, 90.64; Cl2-Mo1-Cl3, 91.04; Cl3-Mo1-S1, 94.18

The coordination sphere of Mo in **1-Cl₃** is approximately octahedral, with the SMoCl₃ unit being almost perfectly planar, although, as is typical with PXP-type pincer ligands, the X-M-P (S-Mo-P) angles are significantly less than 90°, at 76.5±0.5°.

2.2. Reduction of 1-Cl₃ and Binding of N₂. Cyclic voltammetry of **1-Cl₃ in THF** revealed a reversible reduction with a half-wave potential, $E_{1/2} = -1.56$ V vs Fc^{+/0}. This reduction is ca. 400 mV less negative than that of (PNP)MoCl₃ ($E_{1/2} = -1.94$ V vs Fc^{+/0})⁵², confirming our hypothesis that the PSP ligand would support milder reductions. The peak was fully reversible at all scan rates studied, suggesting that chloride dissociation occurs relatively slowly. Chemical reductions

were then attempted with sodium metal, which can assist in chloride abstraction via precipitation of NaCl.

A THF solution of **1-Cl₃** was stirred over Na/Hg amalgam (0.5% w/w Na; 3 equiv Na) under N₂ atmosphere. The predominant product exhibited a very broad AB pattern of doublets δ 80.8 and δ 79.1 in the ³¹P NMR spectrum, ²J_{PP} = ca. 120 Hz. Several other minor signals appeared in the spectrum, including a sharp singlet at δ 78.2. Crystals were obtained and scXRD revealed a dimolybdenum product analogous to Nishibayashi's Mo⁰ dimer [(PNP)Mo(N₂)₂]₂(μ -N₂), ^{22,30-31} i.e. [(PSP)Mo(N₂)₂]₂(μ -N₂) (**2**) (Figure 3; Scheme 2). Note that the bowl shape of the PSP ligand, in contrast with the planar PNP ligand, combined with the orthogonal relationship of the two PSP planes, results in the loss of mirror symmetry, rendering the P atoms of each PSP ligand inequivalent in accord with the predominant species observed in the ³¹P NMR spectrum.

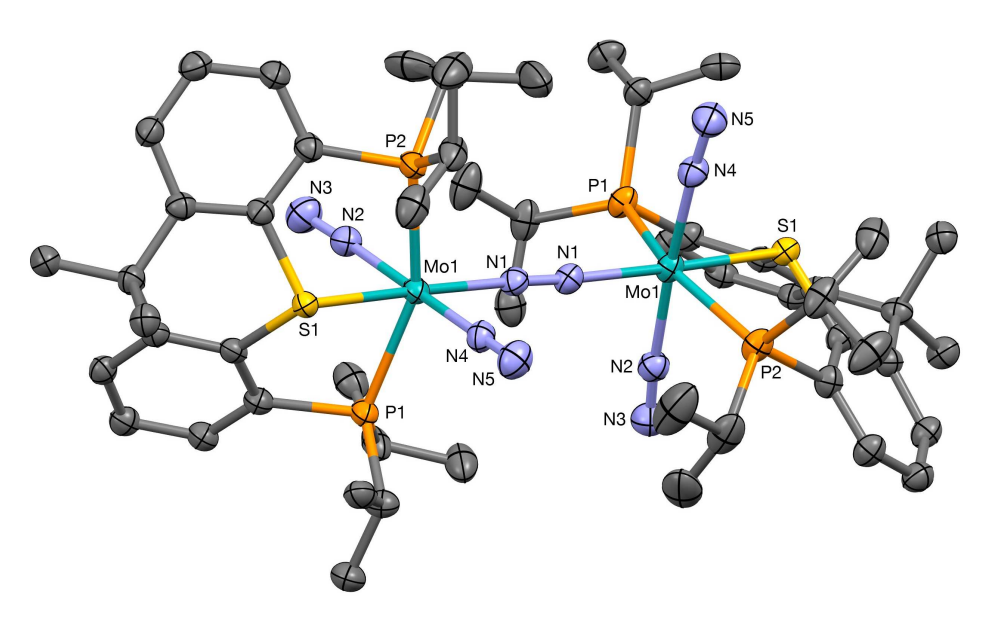


Figure 3. ORTEP representations (50% probability ellipsoids) of the structure of **2** determined by X-ray diffraction; hydrogen atoms and PSP t-butyl groups omitted for clarity. Selected bond lengths (Å) and angles (°): N1-N1, 1.114; Mo1-N1, 2.067; Mo1-N2, 2.044; Mo1-N4, 2.023; N2-N3, 1.109; N4-N5, 1.113; Mo1-P1, 2.447; Mo1-P2, 2.436; P1-Mo1-S1, 79.0; P2-Mo1-S1, 79.5; P1-Mo1-P2, 156.7.

Scheme 2. Reaction of 1-Cl₃ with Na (3 equiv) under N₂ Atmosphere

Redissolving the crystals affords a ^{31}P NMR spectrum similar to that obtained before recrystallization. This leads us to speculate that the unidentified signals may be assigned to one or more isomers of **2** present in equilibrium in solution, e.g. isomers in which the bridging N₂ is positioned cis to S in one or both of the (PSP)Mo units^{21,55-57}. Upon lowering the temperature to 268 K, the AB doublet becomes very well defined with $^2J_{PP}$ = 122.3 Hz. We attribute the singlet at δ 78.2 in the ^{31}P NMR spectrum to a mononuclear product (PSP)Mo(N₂)₃ (**3**). Consistent with this assignment, when N₂ is added to a solution of the mixture, raising the pressure from 1 atm to 6.1 atm N₂, the ratio of the ^{31}P NMR integrals of **3** to **2** increases from 0.7:1 to 5:1 (Scheme 2). Removal of N₂ then results in a decrease of the ratio to 0.2:1.

Admitting a CO atmosphere to the solution of **2** and **3** resulted in a ³¹P NMR spectrum indicating formation of two species, one manifesting a very broad AB doublet (δ 88.8 and δ 88.0), and the other a sharp singlet at δ 91.0. Two products were crystallized from this mixture and both were characterized by scXRD (see SI). One was found to be (PSP)Mo(CO)₃. The other was the N₂-bridging dimer [(PSP)Mo(CO)₂]₂(μ -N₂), which is the analogue of the product of the reaction of [(PNP)Mo(N₂)₂]₂(μ -N₂)^{19,22,30-31} with CO¹⁹.

2.3. Reduction of 1-Cl₃ with Cleavage of N₂. The Mo⁰ dinitrogen complexes described above were stable with regards to the dissociative cleavage reaction to form metal nitrides, as expected based on the number of electrons in π -symmetry orbitals.⁵⁸ A N₂-bridged complex with one less e per Mo would have the appropriate electronic structure for splitting, and iodide additives have previously been found to promote nitride formation in pincer Mo complexes. 30,35,40-41 Accordingly, 1-Cl₃ was treated with two reducing equivalents per Mo, rather than three as in the above examples, in the presence of added iodide. Under N₂ atmosphere, Na/Hg amalgam (0.5% w/w Na; 2 equiv Na) was added to a THF solution of 1-Cl₃ and NaI (2 equiv). The 31 P NMR spectrum of the resulting solution showed a single resonance, at δ 79.8, and the ¹H NMR spectrum was consistent with a single diamagnetic PSP-containing species with C_s symmetry.⁵⁹ When the reaction was conducted under ¹⁵N₂ atmosphere the resulting ¹⁵N NMR spectrum showed a single resonance at δ 446. These spectroscopic data are consistent with assignment as the product of N₂-cleavage, (PSP)Mo(N)I (1-(N)I, Scheme 3). Crystals were grown from benzene/pentane and scXRD afforded the structure shown in Figure 4. The complex 1-(N)I has a coordination geometry that may be viewed as pseudo-square-pyramidal³⁵ with nitride in the apical position and an N-Mo-L angle of ca. 100° with each of the four other Mo-coordinating atoms. This structural motif is well precedented among pincer-Mo^{35,60-61} and related nitride complexes. 62-63

Scheme 3. Reduction of 1-Cl₃ by 2e⁻ under N₂ Atmosphere Leading to Cleavage of N₂

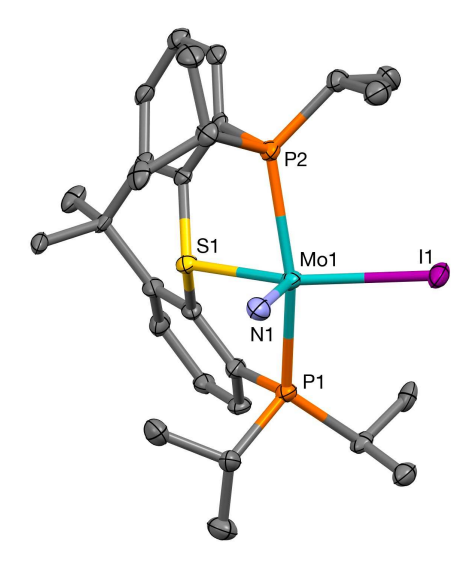


Figure 4. ORTEP representations (50% probability ellipsoids) of the structure of **1-(N)I** determined by X-ray diffraction; hydrogen atoms and PSP *t*-butyl groups omitted for clarity. Selected bond lengths and angles: Mo1-N1, 1.648; Mo1-S1, 2.353; Mo1-I1, 2.815; Mo1-P1, 2.517; N1-Mo1-S1, 101.12; N1-Mo-I1, 107.26; N1-Mo1-P1, 99.73; N1-Mo1-P2, 99.34; P1-Mo1-P2, 152.55; S1-Mo-I1, 151.62

Based on the modest reduction potential of **1-Cl₃** ($E_{1/2} = -1.56$ V vs. Fc^{+/0}), milder reductants should also be viable. Accordingly, under otherwise identical conditions, similar results were obtained with the use of 2 equiv decamethylcobaltocene (Cp*₂Co), which has an oxidation potential of -1.94 V vs. Fc^{+/0}, as reductant in place of Na/Hg amalgam. However, no reaction was obtained with Cp₂Co (-1.33 V vs. Fc^{+/0}).

Thus cleavage of N_2 occurs upon reaction of two equivalents of reductant with **1-Cl₃** while the addition of more than two equivalents leads to a stable bridging- N_2 dimolybdenum(0) complex. This is consistent with the well-established principle that bimetallic cleavage of N_2 to give nitrides is generally limited to bridging- N_2 complexes with 10 electrons in the $M(\mu-N_2)M$ π -system^{12,38,57-58,64-67} (Scheme 4).

Scheme 4. Reduction of 1- X_3 , by 2 e⁻ or 3 e⁻, under N_2 Atmosphere. Hypothetical Pathways to 1-(N)X and 2

$$(PSP)MoX_{3} (1-X_{3}) \\ + 2 e- \\ -2 X^{-} \\ (PSP)Mo^{1}X \\ + e- \\ -X^{-} \\ N_{2} \\ -X^{-} \\ -X^{-} \\ N_{2} \\ -X^{-} \\ -X^{-} \\ -X^{-} \\ N_{2} \\ -X^{-} \\$$

2.4. Protonation of the Nitride Ligand of 1-(N)I. Having observed cleavage of the N₂ bond to give nitride complex **1-(N)I**, we considered likely subsequent steps in a potential catalytic cycle for ammonia synthesis. As will be discussed in depth in following sections, formation of the initial N-H bond is indicated by DFT calculations to be the thermodynamically most challenging step in the conversion of the nitride to ammonia. Accordingly, **1-(N)I** did not react with the H-atom donor TEMPO-H (up to 5 equiv) even after 2 days at room temperature. Nor did **1-(N)I** undergo reaction with one-electron reductants Cp₂Co or Cp*₂Co (1 equiv). We therefore undertook investigation of protonation as the initial N-H bond formation step.

Upon addition of one equiv [LutH][OTf] (the most commonly used proton source in the context of this chemistry³⁰⁻³¹) the characteristic peak of **1-(N)I** in the ³¹P NMR spectrum at δ 79.78 was broadened but only slightly shifted. An extremely broad peak appeared in the ¹H NMR spectrum at ca. δ 14.8. Addition of two more equiv [LutH][OTf] resulted in a shift of the ³¹P NMR signal to δ 78.9, while the downfield ¹H NMR peak shifted to δ 14.7 and became more intense and sharpened. With a total of 12 equiv [LutH][OTf] added, the ³¹P NMR signal appeared at ca. δ 78.2 while the downfield ¹H NMR signal, clearly exchanging with free [LutH][OTf], was at δ 14.5. These results are consistent with protonation of **1-(N)I**, presumably at the nitride ligand, in a rapid equilibrium lying toward the left, either with the triflate anion coordinated to Mo (eq 1a) or ion-paired to the resulting cation (eq 1b). They are also consistent with an equilibrium in which the lutidinium cation is engaged in hydrogen bonding, again presumably with the nitride ligand (eq 1c).

$$1-(N)I + [LutH]^{+}[OTf]^{-} \xrightarrow{} (PSP)Mo(I)(NH)(OTf) + Lut$$
 (1a)

$$\mathbf{1-(N)I} + [LutH]^{+}[OTf]^{-} \stackrel{\longrightarrow}{\longleftarrow} [(PSP)Mo(I)(NH)(Lut)]^{+}[OTf]^{-}$$
(1b)

$$1-(N)I + [LutH]^{+}[OTf]^{-} \leftarrow [(PSP)Mo(I)N \bullet \bullet \bullet HLut]^{+}[OTf]^{-}$$
(1c)

As noted above, the addition of 3 equiv [LutH][OTf] to a solution of **1-(N)I** resulted in a broad signal at δ 78.9 in the ³¹P NMR spectrum. Subsequent addition of 3.0 equiv lutidine essentially returned the chemical shift (δ 79.7) to that of **1-(N)I**; since free lutidine participates only in the

equilibrium of eq 1a, this supports eq 1a over eqs 1b or 1c as a description of the reaction of **1-(N)I** with [LutH][OTf]. Note however that this does not offer insight into the configuration of (PSP)Mo(I)(NH)(OTf), and in particular does not distinguish between an ion pair (likely with OTf-hydrogen bonding to the N-bound proton) versus a complex with OTf-coordinated to molybdenum.

In contrast with the reaction of **1-(N)I** with [LutH][OTf], reaction with Brookhart's acid⁶⁸ [H(Et₂O)₂][BAr^F₄] (Ar^F = 3,5-bis(trimethyl)phenyl) appears to result fully in protonation (eq 2). The ³¹P NMR spectrum shows a single broad signal upon addition of 1.0 equiv [H(Et₂O)₂][BAr^F₄] at δ 67.2. Addition of two more equiv of the acid has no discernible effect on the chemical shift of this signal although the signal is then sharp. Reaction of [H(Et₂O)₂][BAr^F₄] with ¹⁵N-labeled **1-(**¹⁵N)I leads to a doublet (δ 51.0, ¹J_{HN} = 73 Hz) in the ¹⁵N NMR spectrum, which is well precedented in work by Schrock as a protonated nitride.⁶⁹ The ³¹P NMR spectrum of **1-(**¹⁵N)I shows a doublet with a small ³¹P-¹⁵N coupling, ²J_{PN} = 5.8 Hz.

$$(PSP)Mo(I)N + [H(Et_2O)_2][BAr^F_4] \rightarrow [(PSP)Mo(I)NH]^+ [BAr^F_4]^- + 2 Et_2O$$
 (2)

The above results suggest that a very strong acid, such as $[H(Et_2O)_2][BAr^F_4]$, is required to fully protonate **1-(N)I** (to give **1-(NH)I**) while a moderately strong acid, [LutH][OTf], results in an equilibrium (likely with **1-(NH)I(OTf)**) that lies toward the unprotonated form. In contrast with the reaction with [LutH][OTf], however, addition of the chloride salt of the same acid, [LutH][CI](3) equiv), resulted in complete protonation with no observable equilibrium. The ³¹P NMR spectrum indicated the presence of two species in a ca. 4:1 ratio with chemical shifts of δ 63.9 and δ 64.9 respectively. The ¹H NMR spectrum contained signals at δ 6.40 and δ 6.49, also in a ca. 4:1 ratio, attributable to the protonated nitride ligand.

Crystals were grown by diffusion of pentane into a benzene solution. scXRD yielded the molecular structure of *trans*-1-(NH)(Cl)(I) (Figure 5). Apparently, by comparison with lutidinium triflate, in the case of lutidinium chloride coordination of the anion to molybdenum drives protonation of the nitride ligand fully to the protonated form (Scheme 5).

Scheme 5. Protonation of Nitride Ligand of 1-(N)I via Reaction with [LutH]Cl

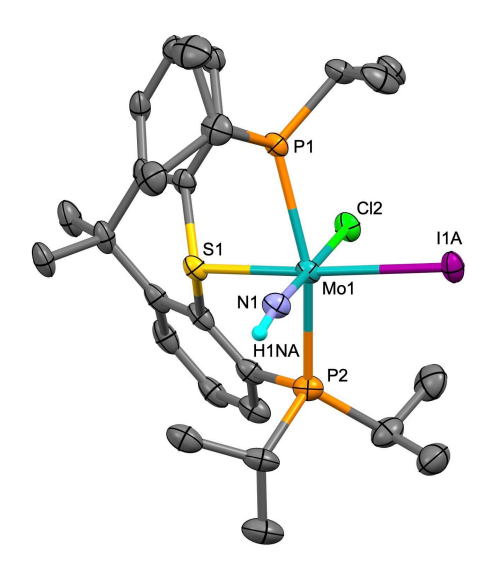


Figure 5. ORTEP representations (50% probability ellipsoids) of the structure of *trans-***1-(NH)(Cl)(I)** determined by X-ray diffraction; hydrogen atoms (other than the imido H), PSP *t*-butyl groups, and minor components of iodide site omitted for clarity. Fixed position of the imido proton determined from electron density map. Selected bond lengths (Å) and angles (°): Mo1-N1, 1.731; Mo1-S1, 2.372; Mo1-I1A, 2.837; Mo1-Cl2, 2.506; Mo1-P1, 2.503; Mo1-P2, 2.496; S1-Mo1-N1, 94.24; N1-Mo-I1A, 96.76; I1A-Mo1-Cl2, 86.44; P1-Mo-S1, 79.41.

We propose that the minor species (with the ^{31}P NMR chemical shift of δ 64.9 and ^{1}H NMR shift of δ 6.49) is the corresponding dichloride complex, (PSP)MoCl₂(NH). In accord with this proposal, the crystal was disordered and the structure was solved as 18% (PSP)MoCl₂(NH).

[LutH]Cl (1.2 equiv) was added to a THF-d₈ solution **1-(**¹⁵**N)l** to yield **1-(**¹⁵**NH)lCl**, which gave a ³¹P{¹H} NMR spectrum with signals, in a 4:1 ratio, at δ 63.5 and δ 64.4, both doublets with ²J_{PN} = 6.1 Hz. The ¹H NMR spectrum revealed a very sharp doublet of triplets at δ 6.31 with ¹J_{NH} = 73 Hz and ³J_{PH} = 3.6 Hz attributable to the major species. In the ¹⁵N NMR spectrum a doublet appears at δ -2.5 (¹J_{NH} = 73 Hz) (the signals were too broad to observe P-N coupling). The HSQC spectrum showed strong correlation of this ¹⁵N signal with the ¹H NMR signal at δ 6.31.

2.5. Reduction of 1-(NH)ICl to Yield Ammonia and the Reverse Reaction. We describe above observations of dinitrogen cleavage and protonation of the resulting nitride ligand. Having accomplished the challenging formation of the first NH bond, it remains to convert imide to ammonia to close a catalytic cycle for ammonia synthesis. This would obviously require reduction and further protonations, or the addition of hydrogen atoms. We next investigated chemistry relevant in this context.

The imido complex **1-(NH)ICI**, in contrast with nitride **1-(N)I**, reacted with the H-atom donor TEMPO-H to give ammonia (Scheme 6). **1-(NH)ICI** was generated in situ by addition of 5 equiv [LutH]Cl to a THF solution (2 mL) of **1-(N)I**; TEMPO-H (8 equiv) was then added and after 24 h the volatiles were removed in vacuo. The residue was dissolved in DMSO-d₆ and ¹H NMR

spectroscopy revealed formation of ammonia (free and/or bound) that was detected as NH_4^+ in 88% yield.

Scheme 6. Reaction of 1-(NH)ICI with TEMPO-H to Yield Ammonia

$$^{t}Bu$$
 $^{pi}Pr_2$
 $^{pi}Pr_2$
 $^{pi}Pr_2$
 $^{pi}Pr_2$
 ^{t}Bu
 ^{t}Bu

Cp₂Co (5 eq) was added, over the course of 12 h, to a solution **1-(NH)ICI** which had been generated by the addition of [LutH]Cl (3 equiv) to a THF-d₈ solution of **1-(N)I**. ¹H NMR spectroscopy revealed appearance of the spectrum characteristic of paramagnetic **1-Cl₃** (which would likely overlap with a mixed halide complex, **1-Cl₂I**) (Scheme 7).

Scheme 7. Reaction of 1-(NH)ICl with [LutH]Cl and Cp₂Co to yield 1-MoCl₃ and NH₃, followed by addition of KO^tBu

Although the stoichiometry of the reaction of Scheme 7 would only require a single equivalent of Cp₂Co, the reaction proceeded rapidly, but not to completion, even upon addition of excess (up to 5 equiv) Cp₂Co. Considering the possibility that an equilibrium had been reached, we investigated the possibility of driving the reaction in reverse. Consistent with our hypothesis, addition of base (KO^tBu, 4 equiv) to the mixture formed in this experiment resulted in the reappearance of the starting material **1-(N)I** (Scheme 7).

The above experiments suggest, rather surprisingly, that the reduction of Mo^{IV} complex **1-(NH)ICI** by Cp_2Co , to give **1-MoCl₃**, Cp_2Co^+ , and presumably ammonia (not observed), is reversible.⁷⁰ Indeed, when $[Cp_2Co][PF_6]$ (3 equiv), NH₃ (2 equiv) and KO^tBu (4 equiv) were added to a fresh solution of **1-Cl₃** in THF-d₈, the formation of Cp_2Co was clearly observed in the ¹H NMR spectrum (δ -50.5) within 18 h. A signal at δ 77.2 in the ³¹P NMR spectrum is attributed to **1-(N)CI** (identified by independent synthesis; see S2.11) (ca. 20% of phosphorus-containing

products). The presumed balanced equation is shown in Scheme 8. The major phosphorus-containing product, however, was the free PSP ligand (ca. 50%).

Scheme 8. Reaction of 1-Cl₃ with NH₃, Base, and Cp₂Co⁺ (Ideal Balanced Equation)

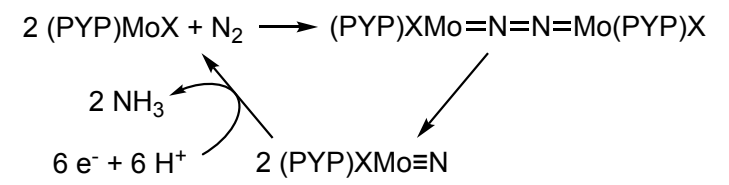
Although individual steps of reduction and N_2 cleavage (Schemes 2-5), and protonation to give ammonium are demonstrated above, we have thus far been unable to achieve a significant level of catalysis with the (PSP)Mo unit. With **1-(N)I** as a prospective catalyst or precursor, the use of various pyridinium hydrohalide derivatives with $Cp*_2Co$ was investigated. Slow addition (over 2 h) of 36 equiv $Cp*_2Co$ to a solution of **1-(N)I** and collidinium triflate (55 eq) under N_2 atmosphere gave 1.29 equiv NH_4^+ ; other attempts generally gave significantly less than one equivalent NH_4^+ . While this may be related to the apparent proclivity of the PSP ligand to dissociate, as illustrated above, efforts are ongoing to more fully characterize the decomposition pathway.

3. COMPUTATIONAL RESULTS AND DISCUSSION OF MECHANISM

The observations described above suggest potential intermediates and reaction steps of a catalytic pathway, proceeding via bimetallic dinitrogen cleavage, for the synthesis of ammonia from dinitrogen (Scheme 9; Y = S). We have attempted to use these observations as points of reference for integration with a computational study of such catalytic cycles. In this study we compare the reactions of the (PSP)Mo fragment with those of the currently best established example of catalysts of this type, the (PNP)Mo-based system reported by Nishibayashi. To further investigate the mechanism of the formation of ammonia, we carried out DFT calculations using the Gaussian 16 (rev. A.03) suite of quantum chemical software.⁷¹ The structures were optimized using the Minnesota-based hybrid metafunctional M06⁷² and Pople's split valence basis set 6-31G(d,p)⁷³⁻⁷⁴ with the Stuttgart-Dresden effective core potential (SDD)⁷⁵ for heavy atoms (Mo, Co, Br, and I). Improved potential energies, which also include some of the effects of bulk solvation, were obtained from single-point calculations of the gas phase optimized geometries employing the M06 functional, the all-electron Karlsruhe basis set Def2-QZVP⁷⁵⁻⁷⁹ for all atoms, and the SMD⁸⁰ dielectric continuum (with benzene as solvent model). The PSP ligand was modeled with an asymmetric derivative bearing t_butylmethylphosphino groups instead of bis(isopropyl)phosphino groups to avoid multiple conformational possibilities, while maintaining the same ligand steric profile.81 Unless explicitly

mentioned, this model has been used for all calculations pertinent to (PSP)Mo halide complexes. Bis(isopropyl)phosphino groups, however, were used for calculations involving the triflate anion to more precisely model the greater steric demands of the triflate ion and the absence of symmetry for triflate-coordinated and especially ion-paired triflate complexes. For the calculation of the inner-sphere reorganization energies associated with the calculation of kinetic barriers of electron transfer, the four-point method was used. The computational methodologies are also discussed, in further detail, in the Supporting Information.

Scheme 9. Proposed Pathway (Highly Simplified) for Catalytic Synthesis of NH_3 via Bimetallic Cleavage of N_2 and Reduction/Protonation



3.1. Cleavage of N₂ by (PSP)Mo. Bimolecular cleavage of N₂ by (PSP)MoX to yield the corresponding nitride complex is central to the mechanism of catalysis implied in this work, in analogy to previous proposals for (PNP)Mo and other (pincer)Mo complexes. ^{12,16,30-34,57,83} In general, in the context of nitrogen fixation, cleavage of the strong N₂ bond is often presented as the origin of the great challenge to achieving conversion under mild conditions. ^{16,30,84-88} The barrier to bimolecular N₂ cleavage, however, is not necessarily particularly high nor ratedetermining. For example, Yoshizawa and Nishibayashi have calculated that the free energy barrier (ΔG^{\ddagger}) to N₂ cleavage by the bridged complex [(PNP)MoI]₂(μ -N₂) is only 21.8 kcal/mol, and that the reaction is exergonic by 27.6 kcal/mol. ²⁷

The N₂-bridging complex [(PSP)MoI]₂(μ -N₂) is calculated to be strikingly similar to its PNP analogue. Although PSP is significantly less electron-donating than PNP (cf. the less negative reduction potential of (PSP)MoCl₃ vs. (PNP)MoCl₃) the bond distance of the bridging N₂ ligand is essentially identical in the two complexes, 1.201 Å and 1.203 Å respectively (D_{NN} = 1.098 Å for free N₂). Likewise the free energy of activation for N₂ cleavage by [(PSP)MoI]₂(μ -N₂) (Scheme 10; X = I), ΔG^{\ddagger} = 21.1 kcal/mol, is essentially equal to that of [(PNP)MoI]₂(μ -N₂), while the reaction is calculated to be somewhat more exergonic (ΔG° = -33.7 kcal/mol). The low activation barrier is consistent with the rapid formation of 1-(N)I observed upon the addition of 2.0 equivalents Na/Hg to 1-Cl₃ under N₂ atmosphere in the presence of NaI (Scheme 3). Slightly greater free energies of activation are calculated for X = Br (ΔG^{\ddagger} = 22.5 kcal/mol) and X = Cl (ΔG^{\ddagger} = 23.7 kcal/mol). The origin of this effect of varying the halide ligand is not obvious, and efforts are currently underway to elucidate it. In all cases the reaction is very exergonic; (ΔG° = -33.4 kcal/mol, -35.6 kcal/mol, -33.7 kcal/mol for X = Cl, Br, I, respectively).

Scheme 10. Activation Barriers and Reaction Energies of Cleavage of the N_2 Bridge of $[(PSP)MoX]_2(\mu-N_2)$; X = CI, Br, I

3.2. (PSP)MoN-H Bond Formation. Given that the barriers to N_2 cleavage are low, and that the reaction is very exergonic (i.e. the nitride products are relatively "low-energy" species), it is very possible that subsequent steps would be rate-determining in any catalytic cycle for the conversion of N_2 to ammonia. This is particularly the case under conditions where the overall free energy of the full cycle for NH_3 formation is not very negative, as would be required to achieve a high level of energy-efficiency¹¹ (most notably, with low overpotential in the case of an electrochemical system). Consistent with the idea of a rate-determining step subsequent to N_2 cleavage, Nishibayashi has proposed that N-H bond formation can be rate-determining in the (PNP)Mo-catalyzed reduction of N_2 to NH_3 . Insight into the reaction of the nitride product to yield NH_3 is therefore critical to a mechanistic understanding of catalytic N_2 reduction pathways and the design of energy-efficient catalysts based on bimetallic N_2 splitting.

Conversion of the nitride ligand to ammonia is also a key segment of catalytic pathways that are based on the so-called distal mechanism for N_2 reduction, first envisioned by Chatt⁸⁹⁻⁹⁰ almost 50 years ago and many years later realized in practice by Yandulov and Schrock.^{18,53,91-92} Indeed, it appears that most molecular catalysts for N_2 reduction based on molybdenum^{19-31,35,93-94} (and very possibly many or most other metals⁹⁵⁻⁹⁶) operate via either bimolecular N_2 -splitting or distal mechanisms; both classes require the conversion of a nitride ligand to ammonia.

The reaction of a metal nitride complex to yield the corresponding fragment plus NH₃ obviously requires the addition of 3 H⁺ and 3 e⁻. It is typically assumed, based on charge balance considerations, that such processes proceed via alternating protonations and reductions. However, the results of our calculations described below, especially when integrated with the experimental results described above, indicate that ammonia formation from the nitride complex (PSP)Mo(N)X, or from its PNP analogue, does not proceed via a simple alternating protonation/reduction pathway.

3.2.1. Formation of the First (PSP)MoN-H Bond. For the conversion of the nitride ligand of (PNP)Mo(N)(I) to a molecule of ammonia, it has been shown that formation of the "first" NH bond is thermodynamically the least favorable of the three sequential bond formation steps; i.e. of the imide, amide, and ammonia complex intermediates, the imide has the lowest N-H

BDFE³⁴. For the (PSP)Mo system we calculate that the respective N-H BDFEs are similar, and in particular that formation of the first N-H bond is likewise the least thermodynamically favorable, by a very significant margin (Table 1; BDFEs of (PYP)MoX[NH₍₁₋₃₎], Y = S, N). The calculated low N-H BDFE is consistent with our experimental observation (Section 2) that TEMPO-H does not undergo reaction with **1-(N)I**.

Table 1. Calculated N-H BDFEs^{a,b} $(PYP)Mo(X)_mNH_{n-1}$ X = CI, I; Y = N, S, m = 1 or 2, n = 1-3

[Mo] = (PSP)Mo	(PSP)MoX[NH ₍₁₋₃₎]			(PSP)MoX ₂ [NH ₍₁₋₃₎]		
	[Mo](X)N-H	[Mo](X)NH–H	[Mo](X)NH ₂ –H	[Mo](X) ₂ N–H	[Mo](X)₂NH−H	[Mo](X) ₂ NH ₂ –H
X = CI	33.0	56.3	51.2	57.9	50.0	55.9
X = I	31.6	58.2	49.3	55.2	49.1	58.3
[Mo] = (PNP)Mo	(PNP)MoXNH ₍₁₋₃₎			(PNP)MoX₂NH ₍₁₋₃₎		
X = CI	31.2	45.0	52.9	53.5	50.7	50.7
X = I	31.9	45.8	51.3	47.9	50.6	51.5

(a) SMD_{benzene}/M06/Def2-QZVP//M06/SDD/6-31G(d,p) (b) values in kcal/mol

In the case of (PNP)Mo(N)X it has been suggested that formation of the first N-H bond may proceed via an initial one-electron reduction²⁷. For **1-(N)X**, however, we calculate that transfer of an electron from $Cp*_2Co$, to give the ion-pair $[Cp*_2Co][(PSP)Mo(N)X]$, is highly endergonic, (35.5, 36.7, and 35.5 kcal/mol for X = Cl, Br, I respectively). (See Computational Section for discussion of ion-pairing effects, without which the electron transfer would be even much more endergonic, calculated as 52.5, 52.8, and 52.2 kcal/mol for X = Cl, Br, I respectively.)

Even before considering the kinetic barrier, the calculated thermodynamic barrier for this one-electron reduction (e.g. ΔG° = 35.5 kcal/mol for X = I) is prohibitively high for a reaction to occur at ambient conditions. Nevertheless, we wished to investigate the kinetic barrier, at least to the extent that computational methods would allow. The reorganization energies (λ_0) were calculated for Cp*₂Co/[Cp*₂Co+] and for (PSP)Mo(N)X/[(PSP)Mo(N)X⁻] and from these values the kinetic barriers to electron transfer could be calculated using the Marcus equation (eq 3).

$$\Delta G^{\ddagger} = \frac{(\lambda_0 + \Delta G^{\circ})^2}{4 \lambda_0}$$
 (3)

The values of ΔG^{\dagger} for reduction of **1-(N)X** by Cp*₂Co were determined, according to eq 3, to be 53.3, 56.5, and 54.2 kcal/mol (X = Cl, Br, I respectively). Clearly these represent a prohibitively high kinetic barrier, but even absent *any* barrier in addition to the calculated endergonicity (e.g. ΔG° = 35.5 kcal/mol for X = Cl, I), the rate at ambient temperature would be extremely slow: 6 x 10⁻¹⁴ s⁻¹ at 25 °C. In agreement with this conclusion, experimentally (Section

2.5), **1-(N)I** underwent no reaction with Cp_2Co or even Cp_2^*Co in the absence of a protonation source e.g. [LutH]CI.

We therefore consider protonation rather than reduction following cleavage of dinitrogen; this has also been proposed for the mechanism of ammonia formation by (PNP)Mo. ⁸³ In the case of (PSP)Mo, as discussed above, we observed that the equilibrium for protonation of N₂ cleavage product **1-(N)(I)** by [LutH][OTf] is slightly unfavorable. In contrast, [LutH]Cl readily reacted to afford an imide complex **1-(NH)(I)(Cl)** without any indication of an observable equilibrium. Our DFT calculations, or at least the relative values for addition of [LutH][OTf] and [LutH]Cl, are consistent with these observations. The reaction of **1-(N)(I)** with [LutH]Cl to give trans-**1-(NH)(Cl)(I)** is calculated to be exergonic, ΔG° = -11.8 kcal/mol (eq 4, X = Cl), whereas the analogous reaction with [LutH][OTf] is very slightly endergonic, ΔG° _{calc} = 0.2 kcal/mol.

(PSP)Mo(N)I + [LutH]X
$$\rightarrow$$
 (PSP)Mo(NH)(I)(X) + Lut X = CI: Δ G° = -11.8 kcal/mol X = OTf: Δ G° = 0.2 kcal/mol (4)

Note that even the calculated endergonic reaction with [LutH][OTf] is promoted by coordination of the corresponding anion (OTf⁻), although less so than in the case of the more strongly coordinating chloride anion. The isomeric N-protonated species without Mo-coordinated triflate (but with triflate hydrogen bonding to the NH ligand) was calculated to be higher in free energy, $\Delta G^{\circ}_{calc} = 7.1$ kcal/mol (eq 5), while unprotonated **1-(N)(I)** hydrogen-bonding to [LutH][OTf] was slightly lower than that, $\Delta G^{\circ}_{calc} = 5.1$ kcal/mol (eq 6), but still higher than the triflate-coordinated product of eq 4. Note that the accuracy of the calculations in comparing energies of neutral species like (PXP)Mo(NH)(I)(OTf) with ion-paired species like (PXP)Mo(I)(NH)*••OTf⁻ may be suspect. For example the solvent continuum model does not account for possible interactions with other species in solution such as additional [LutH][OTf]. Nevertheless, we believe that these results convey the favorability of N-protonation combined with anion coordination and, with more precision, the greater magnitude of this effect ($\Delta\Delta G^{\circ}_{calc} = 11.4$ kcal/mol) with chloride versus triflate anion (eq 4).

(PSP)Mo(N)I + [LutH⁺][OTf⁻]
$$\rightarrow$$
 (PSP)Mo(I)(NH)⁺•••OTf⁻ + Lut $\Delta G^{\circ}_{calc} = 7.1 \text{ kcal/mol}$ (5)

(PSP)Mo(N)I + [LutH⁺][OTf⁻] → [(PSP)Mo(I)(N)•••HLut][OTf]
$$\Delta G^{\circ}_{calc} = 5.1 \text{ kcal/mol}$$
 (6)

The low basicity of the nitride ligand of **1-(N)(I)** is manifest experimentally and computationally in the reaction with [LutH][OTf]. The unfavorable thermodynamics of one-electron reduction of **1-(N)(I)** is experimentally manifest by the lack of reaction even with the strong reductant Cp*₂Co, and this too is in accord with DFT calculations. The very low calculated BDFE of **1-(NH)(I)** is connected to these two factors and is manifest experimentally in the failure of **1-(N)(I)** to react with TEMPO-H. But although these factors might suggest that N-H bond

formation would be challenging, the reaction of **1-(N)(I)** with [LutH]Cl demonstrates experimentally that nitride N-H bond formation can be thermodynamically favorable and very facile—when coupled to the formation of a Mo-X bond (X = a strongly-coordinating anion). Importantly, the same DFT calculations that indicate low basicity, resistance to one-electron reduction, and low N-H BDFE, also yield this same conclusion.

Thus a key finding in this work is that binding a second halide to the Mo center strongly assists the conversion of nitride to imide, i.e. the formation of the "first" NH bond. Absent this halide coordination, formation of this bond is otherwise, by far, the thermodynamically least favorable N-H bond formation on the path from nitride to NH₃. Moreover, the computed N-H BDFE of species 1-(NH)X₂ exceeds 52 kcal/mol, indicating, importantly, that autoformation of H₂ is thermodynamically unfavorable when the additional halide is present. 97 We propose that this very large effect of coordination of the second halide may be attributed in large part to the strong trans influence of the nitride ligand; this trans influence is dramatically reduced upon protonation of the nitride ligand, thus greatly favoring halide addition at the trans position (and, equivalently, halide addition greatly favors nitride-protonation). While the thermodynamics of this effect can be rationalized from different perspectives, we note that it is not simply an electrostatic effect of the negatively charged anion favoring protonation. This point is reflected in the calculation that the N-H BDFEs (Table 1) of the hypothetical species 1-(NH)X₂ are dramatically (by ca. 25 kcal/mol) greater than those of 1-(NH)X, despite both sets of complexes being neutral (Table 1, BDFEs of (PYP)MoX₂[NH₍₁₋₃₎], Y = S). The same effect is seen for the analogous (PNP)Mo complexes (Y = N; Table 1).

We also note (Table 2) that *protonation* of the nitride 1-(N)X is much less favorable than that of imide and amide complexes 1-(N)X and 1-(N)X, and again the same trend is seen for the (PNP)Mo complexes. This further underscores the relative inertness of the nitride ligand formed by N_2 cleavage (Scheme 10). Note however that the basicity of 1-(N) X_2 is comparable to that of 1-(N)X. Thus the additional X ligand does not strongly affect the thermodynamics of protonation (Table 2) but as discussed above, it greatly favors addition of X and X are tribute the latter effect to the removal of one electron from the X0 orbital upon addition of X1 to the Mo center; the resulting half-empty orbital is re-filled upon addition of an X1 atom to the nitride.

Table 2. Calculated energies of N-protonation (relative to N-protonation of 1-(N)(I)) a,b

$H^+ + (PYP)Mo(X)_mNH_n \rightarrow (PYP)Mo(X)_mNH_{n+1}^+ X = CI, I; Y$	' = N, S, m = 1 or 2, n = 0-2
--	---------------------------------

[Mo] = (PSP)Mo	protonation product: (PSP)MoXNH ₍₁₋₃₎ ⁺			protonation product: (PSP)MoX₂NH ₍₁₋₃₎ ⁺		
	[Mo](X)N-H+	[Mo](X)NH-H+	[Mo](X)NH ₂ –H+	[Mo](X) ₂ N-H+	[Mo](X) ₂ NH–H+	[Mo](X) ₂ NH ₂ -H+
X = CI	-0.7	-14.6	-18.5	+0.1	+1.0	-17.3
X = I	[0.0]	-14.2	-13.8	+3.7	+3.1	-17.6
[Mo] = (PNP)Mo	protonation product: (PNP)MoXNH ₍₁₋₃₎ +			protonation product: (PNP)MoX₂NH ₍₁₋₃₎ ⁺		
X = CI	-3.6	-20.2	-29.2	-1.1	-2.2	-18.8
X = I	-3.8	-18.9	-26.5	+7.8	-0.0	-20.9

(a) SMD_{benzene}/M06/Def2-QZVP//M06/SDD/6-31G(d,p) (b) values in kcal/mol

3.2.2. Formation of the Second N-H Bond ((PSP)MoNH-H). Our initial experimental observations of N-H bond formation involved the reaction of the iodide complex 1-(N)(I) with the lutidinium chloride salt. For the purpose of analyzing a multi-step pathway, however, mixing halides complicates an already complicated set of possibilities with multiple possible permutations including isomers and halide exchange products. In the following discussion of the full conversion of nitride to NH₃ we will therefore consider the reaction of (PSP)Mo(N)(CI) with [LutH]CI (3 equiv). The complete and fully analogous pathways have also been calculated for the reactions of (PSP)Mo(N)(I) with [LutH]I and (PSP)Mo(N)(Br) with [LutH]Br, in both cases favoring the same pathway as obtained with chlorides, and thereby yielding the same conclusions. We have also calculated pathways for further N-H bond formation with [LutH][OTf] subsequent to the reaction of 1-(N)(I) with [LutH][OTf] to yield 1-(NH)(I)(OTf). (See Supporting Information).

In a conventional framework of alternating protonation/reduction, one-electron reduction would be expected to follow protonation of the nitride ligand, based on a need to preserve charge balance. However, in the case of protonation of **1-(N)X** this cannot be assumed, as charge balance is maintained by addition of a second halide. Following the net addition of HCl to **1-(N)Cl**, transfer of an electron from Cp*₂Co to **1-(NH)Cl**₂, to give the ion-pair [Cp*₂Co][(PSP)Mo(NH)Cl₂], is in fact calculated to be highly endergonic, $\Delta G^{\circ} = 28.7$ kcal/mol (eq 7, and Pathway **A** in Figure 6).

$$Cp*_{2}Co + (PSP)Mo(NH)X_{2} \rightarrow [Cp*_{2}Co^{+}][(PSP)Mo(NH)X_{2}^{-}] X = Cl; \Delta G^{\circ} = 28.7 \text{ kcal/mol} (7)$$

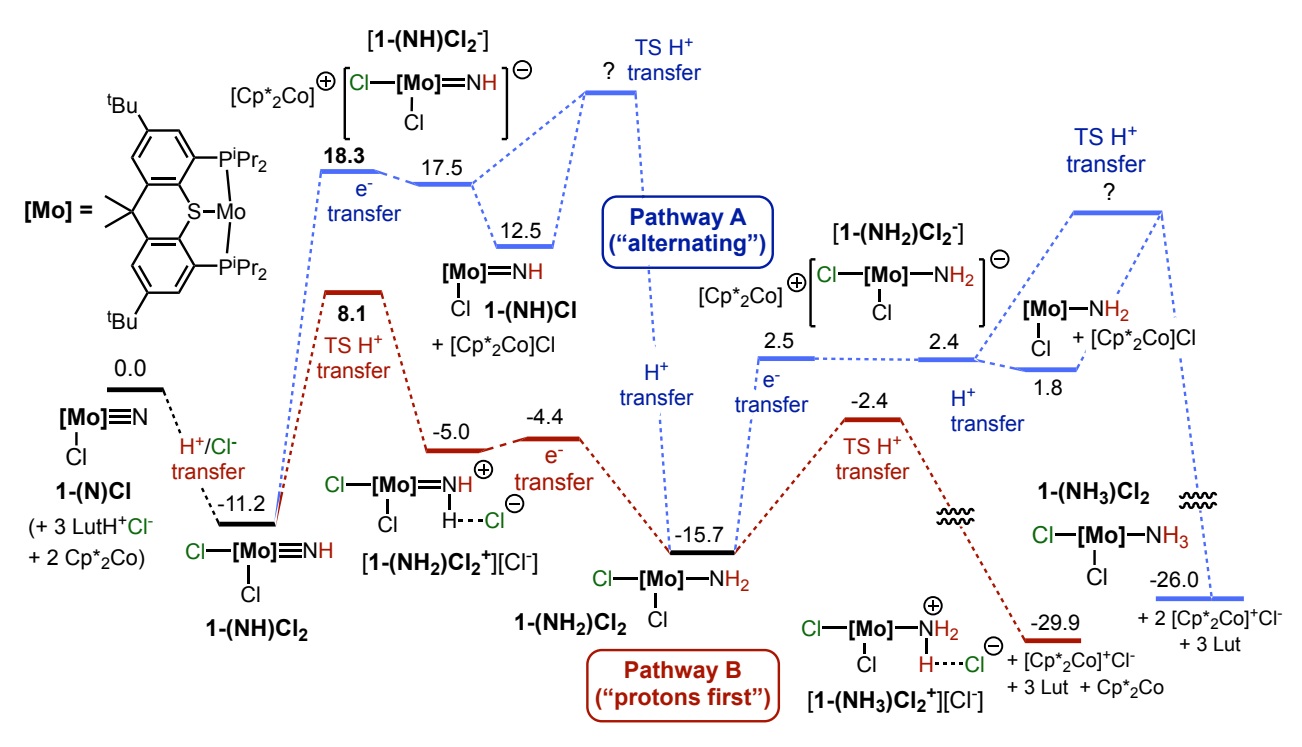


Figure 6. Gibbs free energy profile (kcal/mol) for calculated pathways for the conversion of the nitride ligand of (PSP)Mo(N)Cl to ammonia (the formation of three N-H bonds). The "protons-first" pathway (red), comprising the addition of Cl⁻, three H⁺, and one e⁻, has an overall barrier at least 9.5 kcal/mol less than that of the "alternating" pathway (blue), addition of H⁺(Cl⁻)/e⁻/H⁺/e⁻/H⁺ (i.e. PT-ET-PT-ET-PT)

Using the same Marcus-theory based approach as described above to estimate the kinetics of one-electron reduction of **1-(N)X**, ΔG^{\ddagger} for reduction of **1-(NH)Cl**₂ by Cp*₂Co was determined to be 28.8 kcal/mol (Figure 6, Pathway **A**). Given the limitations of Marcus theory⁹⁸⁻⁹⁹ and assuming that the thermodynamic value of ΔG° = 28.7 kcal/mol must be viewed as a calculated lower limit, we suspect that the kinetics of the electron transfer step would be slower than are indicated by this calculated value of ΔG^{\ddagger} . Nevertheless even the rate predicted based upon the assumption that ΔG^{\ddagger} = 28.8 kcal/mol would be prohibitively slow at ambient temperature (5 x 10^{-9} s⁻¹ at 25 °C).

Subsequent loss of chloride from the hypothetical ion-paired product of electron-transfer, $[Cp*_2Co^+][(PSP)Mo^{|||}(NH)Cl_2^-]$, is calculated to be exergonic by 5.0 kcal/mol (Figure 6, Pathway A; eq 8b), leading to the formation of (PSP)Mo(NH)Cl and $[Cp*_2Co]Cl$. The overall reduction is shown in eq 8c.

$$(PSP)Mo^{IV}(NH)Cl_2 + Cp*_2Co^+][(PSP)Mo^{II}(NH)Cl_2^-] \qquad \Delta G^\circ = 28.7 \text{ kcal/mol} \qquad (8a)$$

$$[Cp*_2Co^+][(PSP)Mo^{|||}(NH)Cl_2^-] \rightarrow (PSP)Mo^{|||}(NH)Cl + [Cp*_2Co^+]Cl^- \Delta G^\circ = -5.0 \text{ kcal/mol}$$
 (8b)

$$(PSP)Mo^{IV}(NH)Cl_2 + Cp*_2Co \rightarrow (PSP)Mo^{III}(NH)Cl + [Cp*_2Co^+]Cl^- \qquad \Delta G^\circ = 23.7 \text{ kcal/mol} \qquad (8c)$$

We calculate that if (PSP)Mo^{III}(NH)CI (**1-(NH)CI**) were formed it could react with [LutH]Cl to undergo addition of HCl across the Mo^{III}=NH bond (similarly to the initial addition of HCl across the Mo-N bond of (PSP)Mo^{III}(N)Cl) leading to amido complex (PSP)Mo^{III}(NH₂)Cl₂ (eq 9 and Figure 6, Pathway **A**). The TS for the proton transfer from lutidinium chloride could not be located but even assuming that there is a negligible enthalpic barrier, the entropic contribution of a bimolecular reaction is expected to be significant (and similar to the high barrier determined for the (PNP)Mo system which is discussed below). Thermodynamically, the reaction of **1-(NH)CI** with [LutH]Cl (eq 9) is calculated to be exergonic by 28.2 kcal/mol (Figure 6, Pathway **A**). Eqs 8 and 9 combine to give a reduction-first pathway for the net addition of H-atom to the imide nitrogen of **1-(NH)CI**₂ to give **1-(NH₂)CI**₂.

$$(PSP)Mo^{III}(NH)CI + [LutH]CI \rightarrow (PSP)Mo^{III}(NH2)CI2 + Lut \Delta G^{\circ} = -28.2 \text{ kcal/mol}$$
(9)

An alternative pathway, much more kinetically favorable than that of eqs 8 and 9, has been calculated as shown in Pathway **B** in Figure 6. Following the reaction of the nitride complex **1-(N)Cl** with [LutH]Cl to give **1-(NH)Cl**₂, a second protonation, the reaction of **1-(NH)Cl**₂ with [LutH]Cl (eq 10) is calculated to be endergonic by only 6.2 kcal/mol (Pathway **B**). The kinetic barrier for this second protonation is calculated be ΔG^{\ddagger} = 19.3 kcal/mol (mostly attributable to entropy, since ΔE^{\ddagger} is only 7.3 kcal/mol), which would allow a very rapid reaction at room temperature.

1-(NH)Cl₂ + [LutH⁺]Cl⁻ → [**1-(NH₂)Cl₂⁺**]Cl⁻ + Lut (10)

$$\Delta G^{\dagger} = 19.3 \text{ kcal/mol}; \Delta G^{\circ} = 6.2 \text{ kcal/mol}$$

Reduction of the protonated complex $[1-(NH_2)Cl_2]^+Cl^-$ is calculated to be exergonic, $\Delta G^\circ = -10.7$ kcal/mol (eq 11; Figure 6, Pathway B). Employing Marcus theory as discussed above, the kinetic barrier to electron transfer is determined to be very low, $\Delta G^\dagger = 0.6$ kcal/mol.

[1-(NH₂)Cl₂+]Cl⁻ + Cp*₂Co
$$\rightarrow$$
 [Cp*₂Co⁺]Cl⁻ + 1-(NH₂)Cl₂ (11)

$$\Delta G^{\dagger} = 0.6 \text{ kcal/mol}; \Delta G^{\circ} = -10.7 \text{ kcal/mol}$$

Thus, conversion of nitride complex **1-(N)Cl** to **1-(NH₂)Cl₂** proceeds initially via N-protonation combined with addition of halide to Mo, as a rapid exergonic reaction to yield **1-(NH)Cl₂**. **1-(NH)Cl₂** then undergoes a slightly endergonic, protonation (eq 10). Reduction of the protonated complex by Cp^*_2Co is calculated to be exergonic with a very low kinetic barrier (eq 11). The reactions of **1-(N)X** with [LutH]X to give **1-(NH)X₂** are calculated to be very comparably favorable for X = Br and I, as are the subsequent protonations to give [**1-(NH₂)X₂**⁺]X⁻. Reduction by Cp^*_2Co subsequent to the second protonation is slightly more favorable for X = Br (ΔG° =

-11.7 kcal/mol) and slightly more so for X = I (ΔG° = -13.3 kcal/mol). In the case of the reaction of **1-(N)I** with [LutH][OTf], while the initial protonation/anion-coordination is less favorable (ΔG° = 0.2 kcal/mol), the second protonation has an energy (ΔG° = 4.3 kcal/mol) similar to eq 10, and the subsequent reduction by Cp*₂Co is more favorable (ΔG° = -17.4 kcal/mol) than eq 11.

Experimentally, consistent with the prediction of a very facile (and not rate-limiting) reduction by $Cp^*{}_2Co$, even with use of the much weaker reductant Cp_2Co (Scheme 7), the formation of the second (as well as third) N-H bonds proceeds readily. With Cp_2Co , a hypothetical reduction of **1-(NH)Cl**₂ prior to protonation would be even more endergonic, significantly, than with $Cp^*{}_2Co$ ($\Delta E^\circ = 0.61 \text{ eV} = 14.1 \text{ kcal/mol}$, neglecting differences in ion-pairing energies). The "protons first" pathway (Figure 6, Pathway B) is thus strongly favored, by computation and experiment, for the formation of the first two N-H bonds on the path of the conversion of nitride ligand to ammonia. The preference for Pathway B is expected to apply even more strongly with any reducing agent weaker than $Cp^*{}_2Co$ or, in the case of an electrochemical system, if the cathodic overpotential is not very high.

3.2.3. Formation of the Third N-H Bond ((PSP)MoNH₂-H). Following formation of amido complex **1-(NH₂)Cl₂**, the "alternating motif" (Figure 6, Pathway **A**) would involve one-electron reduction followed by a third protonation. Reduction of **1-(NH₂)Cl₂** by Cp*₂Co is calculated to be endergonic by 18.1 kcal/mol, with a kinetic barrier calculated (using Marcus theory) to be 18.2 kcal/mol (Figure 6). Again, we were unable to locate a transition state for protonation of the resulting anion to give **1-(NH₃)Cl₂** but again the unfavorable entropy of a bimolecular reaction would result in a significant addition to the barrier. But even compared with only the free energy (Δ G°) of the electron transfer, the calculated kinetic barrier to protonation of **1-(NH₂)Cl₂** is lower, Δ G[‡] = 13.3 kcal/mol and the reaction is highly exergonic (Δ G° = -14.2 kcal/mol; Figure 6, Pathway **B**); protonation of **1-(NH₂)Cl₂** will therefore be rapid, affording the cationic ammonia complex [**1-(NH₃)Cl₂**]+Cl⁻. The calculated reaction barriers and free energies are very similar for the reactions of **1-(NH₂)X₂** to give [**1-(NH₃)X₂**+]X⁻ for X = Br (Δ G° = -15.8 kcal/mol) and X = I (Δ G° = -16.7 kcal/mol) (see Supporting Information).

As discussed above in regard to formation of the second N-H bond, the observation that formation of the third N-H bond proceeds readily even with the Cp_2Co instead of Cp^*_2Co argues that a reduction step does not contribute to a rate-determining barrier; again this is consistent with a "protons first" pathway (Figure 6, Pathway B). Beginning with (PSP)Mo(N)X (1-(N)X), the overall pathway to NH₃ formation may therefore be described as addition of H⁺/X⁻/H⁺/e⁻/H⁺.

Subsequent to the very exergonic third protonation via pathway \mathbf{B} , displacement of NH₃ by Cl⁻ (Scheme 11) is calculated to be exergonic by 10.5 kcal/mol, giving $\mathbf{1}\text{-Cl}_3$, the complex with which we began our study. In a catalytic cycle, if this displacement of ammonia by chloride occurs it would necessarily be followed by one-electron reduction and loss of a halide ion (Scheme 11) – the presumed initial step in the reactions of Schemes 2 and 3. An alternative to the replacement of NH₃ by chloride (and subsequent reduction), would be direct one-electron reduction of the

cationic species [1-(NH₃)Cl₂]⁺Cl⁻ (Scheme 11). This step leads to the last species shown to be formed in Pathway A in Figure 6, i.e. the neutral Mo^{II} complex 1-(NH₃)Cl₂, but with an overall free energy of activation much lower than that of Pathway A (which proceeds via one-electron reduction of neutral 1-(NH₂)Cl₂). Although beyond the scope of this work, further investigations are underway to determine in detail the pathways for reduction, with chemical reductants and electrochemically, which ultimately lead from Mo^{III} complexes [1-(NH₃)X₂⁺] to the N₂-bridging dimolybdenum(I) complexes [(PSP)MoX](μ -N₂).

Scheme 11. Alternative Pathways for Loss of NH₃ and Reduction by Cp*₂Co, Subsequent to Protonation of 1-(NH₂)Cl₂ by [LutH]Cl

3.3. (PNP)MoN-H Bond Formation. Extending our computational approach to the iconic PNP system yields results that are strikingly similar to those obtained for PSP. As in the case of the PSP system, the initial N-H bond formation, using [LutH]Cl as the source of H⁺, is calculated to be exergonic (by 5.9 kcal/mol) when coupled with chloride coordination. This reaction appears to have no barrier on the electronic energy surface. A subsequent hypothetical one-electron reduction by $Cp^*{}_2Co$ is endergonic by 26.5 kcal/mol (Pathway A, Figure 7). For protonation of the resulting anion, in contrast with the case of the PSP analogue ([(PSP)Mo(NH)Cl₂]⁻ anion), we successfully located a transition state; the free energy is 11.3 kcal/mol above the ion pair (fully attributable to entropy). The overall barrier to e⁻-transfer followed by protonation is therefore prohibitively high, 36.7 kcal/mol. In contrast, protonation of (PNP)Mo(NH)Cl₂ is slightly exergonic ($\Delta G^{\circ} = -2.0$ kcal/mol), with a relatively low barrier $\Delta G^{\dagger} = 21.2$ kcal/mol. One-electron reduction of the resulting [(PNP)Mo(NH₂)Cl₂⁺]Cl⁻ ion pair is also slightly exergonic, and with a very low calculated kinetic barrier of $\Delta G^{\dagger} = 1.6$ kcal/mol as determined using Marcus theory (Pathway B, Figure 7).

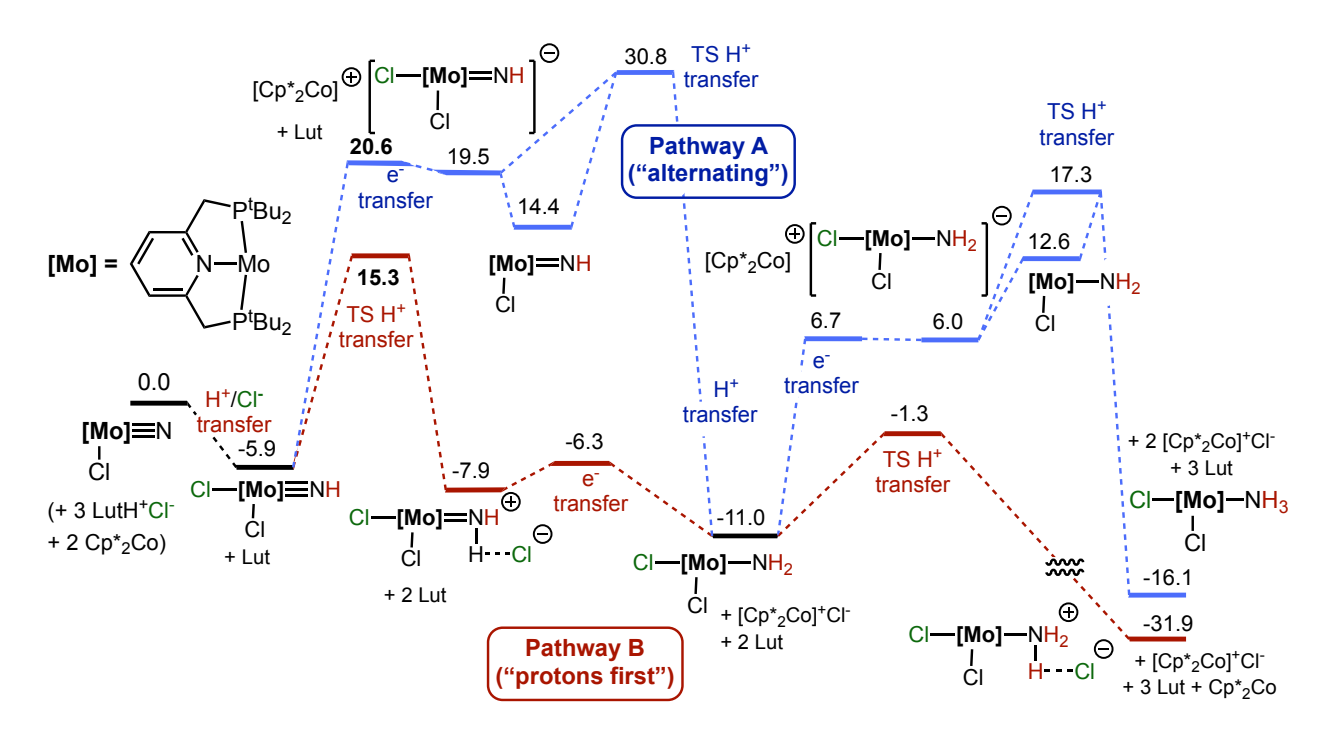


Figure 7. Free energy profile (kcal/mol) for the two calculated pathways for the conversion of the nitride ligand of (PNP)Mo(N)Cl to ammonia (the formation of three N-H bonds). The "protons-first" pathway (red), comprising the addition of three H⁺ and one e⁻, has an overall barrier that is 15.5 kcal/mol less than that of the "alternating" pathway (blue), addition of H⁺/e⁻/H⁺/e⁻/H⁺.

The "protons first" Pathway $\bf B$ and the "alternating" Pathway $\bf A$ reach the common intermediate (PNP)Mo(NH₂)Cl₂ analogously to the (PSP)Mo system. In the (PNP)Mo case our ability to locate a TS for the second protonation allows us to more quantitatively determine that the overall barrier for Pathway $\bf A$ is significantly higher, by 15.5 kcal/mol) (30.8 kcal/mol versus 15.3 kcal/mol) than that for Pathway $\bf B$ (Figure 7).

The intermediate common to both Pathways **A** and **B** in Figure 7, (PNP)Mo(NH₂)Cl₂, can undergo either protonation or reduction. As in the case of the (PSP)Mo system the barrier to reduction is not prohibitive, but protonation is much more favorable than reduction, kinetically ($\Delta G^{\ddagger} = 9.7 \text{ kcal/mol vs. } 17.7 \text{ kcal/mol}$) and especially thermodynamically ($\Delta G^{\circ} = -20.9 \text{ kcal/mol vs. } 17.0 \text{ kcal/mol}$). Moreover, as with formation of the second N-H bond, we have successfully located a TS for protonation subsequent to reduction (again, in contrast with the (PSP)Mo system) to form the third N-H bond. The overall barrier for the net addition of H-atom to (PNP)Mo(NH₂)Cl₂ via the reduction/protonation pathway is 28.3 kcal/mol. This compares with the much lower barrier of $\Delta G^{\ddagger} = 9.7 \text{ kcal/mol for the very exergonic protonation yielding bound ammonia to afford the cationic complex [(PNP)Mo(NH₃)Cl₂+]. Our calculations with the PNP ligand thus serve both to place the conclusions with PSP on firmer ground, and to indicate the generalizability of these results.$

4. CONCLUSIONS

Pincer-molybdenum complexes, most notably Nishibayashi's (PNP)Mo-based and related, have demonstrated great promise as catalysts for the formation of NH_3 from N_2 under mild conditions. As reported in this work, analogous (PSP)Mo complexes have been synthesized and their reactivity has been explored, including the observation of intermediates and stochiometric reactions directly relevant to this class of catalysts. In particular, our isolation of a nitride resulting from the cleavage of N_2 and the formation and characterization of the corresponding imido complexes may offer general mechanistic insight into various N_2 reduction pathways proceeding via such intermediates.

Experimentally, the reaction of **1-Cl₃** with an excess of reductant leads to the stable bridging-nitrogen complex **2**, while reaction with only two equivalents Na/Hg per Mo in the presence of NaI leads to facile cleavage of N_2 to give nitride complex **1-(N)(I)**. The very strong acid $[H(Et_2O)_2][BAr^F_4]$ protonates the nitride ligand of **1-(N)(I)**. Reaction with the moderately strong acid [LutH][OTf], which is often used for catalytic N_2 -to-NH₃ conversion systems of this type, results in an equilibrium that lies toward unprotonated **1-(N)(I)**, with a product that is not definitively characterized. [LutH]CI, however, readily reacts with **1-(N)(I)**, protonating the nitride ligand and adding chloride to the Mo center to give the fully characterized product **1-(NH)(I)(CI)**. In the presence of additional [LutH]CI this Mo^{IV} complex can then be reduced, even with the relatively weak reducing agent, Cp_2Co , (Scheme 7) resulting in the formation of NH₃ and Mo^{III} complex **1-Cl₃**. This reaction appears to reach equilibrium, and if base is added the reverse reaction is observed.

The results of DFT calculations are consistent with and shed light on various experimental observations, and their implications appear to apply to the (PNP)Mo analogues as well. Cleavage of N_2 by the reduced Mo^I fragment to give the nitride complex $\mathbf{1}$ - $(\mathbf{N})(\mathbf{I})$ is calculated to be kinetically facile and thermodynamically favorable in accord with experimental results. The N-H BDFE of the corresponding imide $\mathbf{1}$ - $(\mathbf{N}+\mathbf{H})(\mathbf{I})$ is particularly low and therefore its formation is intrinsically the least favorable of the three N-H bond formations leading to ammonia. Accordingly, the H-atom transfer reagent TEMPO-H does not undergo reaction with $\mathbf{1}$ - $(\mathbf{N})(\mathbf{I})$; nor does $\mathbf{1}$ - $(\mathbf{N})(\mathbf{I})$ undergo reduction by $\mathbf{Cp}^*_2\mathbf{Co}$. However, in agreement with experiment, protonation of the nitride ligand of $\mathbf{1}$ - $(\mathbf{N})(\mathbf{I})$ by [LutH]CI, in combination with addition of the chloride anion at the trans position to yield $\mathbf{1}$ - $(\mathbf{N}+\mathbf{I})(\mathbf{I})(\mathbf{I})(\mathbf{I})$, is computed to be kinetically facile and thermodynamically favorable.

Thus a key conclusion of this work is that the addition of H-X circumvents the unfavorable formation of the "first N-H bond" by coupling addition of H⁺ to the nitride ligand with addition of X⁻ to Mo. We note that nitride protonation not only results in a positive charge on the complex but it is also expected to greatly reduce the trans influence of the nitride ligand; both of these factors strongly favor the coupling of protonation with addition of halide. Alternatively, from a purely thermodynamic perspective, one may view the net addition of H-X as addition of H•

coupled with addition of CI•. The addition of CI• would oxidize the Mo^{IV} center of **1-N(X)** to Mo^V; the resulting half-empty orbital receives the electron of H• upon its addition to the nitride ligand.

Regarding formation of the following two N-H bonds, calculations indicate that conversion of $\mathbf{1}$ -(NH)X₂ to $\mathbf{1}$ -(NH₂)X₂ (i.e. net addition of an H atom to the imide ligand) proceeds through a slightly endergonic protonation by [LutH]X followed by a kinetically very facile reduction by Cp*₂Co. A final protonation by [LutH]X to give [$\mathbf{1}$ -(NH₃)X₂+]X⁻, is calculated to be kinetically facile and very exergonic for X = Cl, Br, I. Thermodynamically, the overall reaction of $\mathbf{1}$ -(NH)X₂ with Cp₂Co and [LutH]X to yield this ammonia complex is calculated to be only slightly exergonic; this is consistent with the experiments indicating that the reaction of $\mathbf{1}$ -(NH)(I)(CI) with Cp₂Co and [LutH]Cl to give NH₃ and Cp₂Co+ is reversible.

Alternative pathways subsequent to the initial addition of H-X to 1-N(X) or to (PNP)Mo(N)(X) cannot be ruled out. Concerted PCET mechanisms in particular must be considered. However, the calculations – consistent with all relevant experimental observations – strongly indicate that the "protons-first" route is kinetically viable and much more favorable than an "alternating" pathway in which successive reductions are followed by protonation. Thus the overall sequence of N_2 reduction appears to proceed through cleavage to yield nitride, followed by addition of $H^+/X^-/H^+/e^-/H^+$ to yield coordinated NH_3 .

Accession Codes

CCDC 2280371, 2329048, 2340506-2340509 contain the supplementary crystallographic data for this paper. These data can be obtained free of charge via www.ccdc.cam.ac.uk/data_request/cif, or by emailing data_request@ccdc.cam.ac.uk, or by contacting The Cambridge Crystallographic Data Centre, 12 Union Road, Cambridge CB2 1EZ, UK; fax: +44 1223 336033.

■ AUTHOR INFORMATION

Corresponding Author

Alan S. Goldman – Department of Chemistry and Chemical Biology, Rutgers, The State University of New Jersey, New Brunswick, New Jersey 08854, United States; orcid.org/0000-0002-2774-710X; Email: alan.goldman@rutgers.edu

Authors

- **Santanu Malakar** Department of Chemistry and Chemical Biology, Rutgers, The State University of New Jersey, New Brunswick, New Jersey 08854, United States; https://orcid.org/0000-0002-3838-5095
- **Souvik Mandal** Department of Chemistry and Chemical Biology, Rutgers, The State University of New Jersey, New Brunswick, New Jersey 08854, United States; https://orcid.org/0000-0003-2402-6662
- **Xiaoguang Zhou** Department of Chemistry and Chemical Biology, Rutgers, The State University of New Jersey, New Brunswick, New Jersey 08854, United States; https://orcid.org/0000-0001-7675-6216
- **Quinton Bruch** Department of Chemistry, University of North Carolina at Chapel Hill, Chapel Hill, North Carolina 27599-3290, United States; https://orcid.org/0000-0002-3653-1036
- **Rachel Allen** Department of Chemistry and Chemical Biology, Rutgers, The State University of New Jersey, New Brunswick, New Jersey 08854, United States; https://orcid.org/0009-0003-1244-2666
- **Laurence W. Giordano** Department of Chemistry and Chemical Biology, Rutgers, The State University of New Jersey, New Brunswick, New Jersey 08854, United States; https://orcid.org/0000-0002-4624-4444
- Nicholas J. I. Walker Department of Chemistry and Chemical Biology, Rutgers, The State University of New Jersey, New Brunswick, New Jersey 08854, United States; https://orcid.org/0009-0004-9423-8366
- **Thomas J. Emge** Department of Chemistry and Chemical Biology, Rutgers, The State University of New Jersey, New Brunswick, New Jersey 08854, United States; https://orcid.org/0000-0003-4685-8419
- **Faraj Hasanayn** Department of Chemistry, American University of Beirut, Beirut 1107 2020, Lebanon; https://orcid.org/0000-0003-3308-7854
- **Alexander J. M. Miller** Department of Chemistry, University of North Carolina at Chapel Hill, Chapel Hill, North Carolina 27599-3290, United States; https://orcid.org/0000-0001-9390-3951

Complete contact information is available at: https://pubs.acs.org/10.1021/jacs.xxxxx

Notes

The authors declare no competing financial interests.

■ **ACKNOWLEDGMENTS**. This work was supported through the National Science Foundation Chemical Catalysis program under Grants No. CHE-2247259 and CHE-2247257, and through the NSF MRI Program, Award 2117792. Additional support was provided by the Alwaleed Center for American Studies and Research at AUB.

References

- (1) Smil, V. *Enriching the Earth: Fritz Haber, Carl Bosch, and the Transformation of World Food Production*; MIT Press: Cambridge, MA, 2004.
- (2) Erisman, J. W.; Sutton, M. A.; Galloway, J.; Klimont, Z.; Winiwarter, W. How a century of ammonia synthesis changed the world *Nat. Geosci.* **2008**, *1*, 636-639.
- (3) Rafiqul, I.; Weber, C.; Lehmann, B.; Voss, A. Energy efficiency improvements in ammonia production—perspectives and uncertainties *Energy* **2005**, *30*, 2487-2504.
- https://www.sciencedirect.com/science/article/pii/S0360544204004943
- (4) Giddey, S.; Badwal, S. P. S.; Munnings, C.; Dolan, M. Ammonia as a Renewable Energy Transportation Media *ACS Sustain. Chem. Eng.* **2017**, *5*, 10231-10239. https://doi.org/10.1021/acssuschemeng.7b02219
- (5) Del Castillo, T. J.; Thompson, N. B.; Peters, J. C. A Synthetic Single-Site Fe Nitrogenase: High Turnover, Freeze-Quench ⁵⁷Fe Mössbauer Data, and a Hydride Resting State *J. Am. Chem. Soc.* **2016**, *138*, 5341-5350. http://pubs.acs.org/doi/abs/10.1021/jacs.6b01706
- (6) Singh, A. R.; Rohr, B. A.; Schwalbe, J. A.; Cargnello, M.; Chan, K.; Jaramillo, T. F.; Chorkendorff, I.; Nørskov, J. K. Electrochemical Ammonia Synthesis—The Selectivity Challenge *ACS Catal.* **2017**, *7*, 706-709. https://doi.org/10.1021/acscatal.6b03035
- (7) Foster, S. L.; Bakovic, S. I. P.; Duda, R. D.; Maheshwari, S.; Milton, R. D.; Minteer, S. D.; Janik, M. J.; Renner, J. N.; Greenlee, L. F. Catalysts for nitrogen reduction to ammonia *Nat. Catal.* **2018**, *1*, 490-500. https://doi.org/10.1038/s41929-018-0092-7
- (8) Chen, J. G.; Crooks, R. M.; Seefeldt, L. C.; Bren, K. L.; Bullock, R. M.; Darensbourg, M. Y.; Holland, P. L.; Hoffman, B.; Janik, M. J.; Jones, A. K.; Kanatzidis, M. G.; King, P.; Lancaster, K. M.; Lymar, S. V.; Pfromm, P.; Schneider, W. F.; Schrock, R. R. Beyond fossil fuel–driven nitrogen transformations *Science* **2018**, *360*, eaar6611. https://www.science.org/doi/10.1126/science.aar6611
- (9) Suryanto, B. H. R.; Du, H.-L.; Wang, D.; Chen, J.; Simonov, A. N.; MacFarlane, D. R. Challenges and prospects in the catalysis of electroreduction of nitrogen to ammonia *Nat. Catal.* **2019**, *2*, 290-296.
- (10) Guo, W.; Zhang, K.; Liang, Z.; Zou, R.; Xu, Q. Electrochemical nitrogen fixation and utilization: theories, advanced catalyst materials and system design *Chem. Soc. Rev.* **2019**, *48*, 5658-5716. http://dx.doi.org/10.1039/C9CS00159J
- (11) Hochman, G.; Goldman, A. S.; Felder, F. A.; Mayer, J. M.; Miller, A. J. M.; Holland, P. L.; Goldman, L. A.; Manocha, P.; Song, Z.; Aleti, S. The Potential Economic Feasibility of Direct Electrochemical Nitrogen Reduction as a Route to Ammonia *ACS Sustain. Chem. Eng.* **2020**, *8*, 8938–8948. https://doi.org/10.1021/acssuschemeng.0c01206 (12) Bruch, Q. J.; Connor, G. P.; McMillion, N.; Goldman, A. S.; Hasanayn, F.; Holland, P. L.; Miller, A. J. M. Considering Electrocatalytic Ammonia Synthesis via Bimetallic Dinitrogen Cleavage *ACS Catal.* **2020**, *10*, 10826–10846. https://doi.org/10.1021/acscatal.0c02606
- (13) Chalkley, M. J.; Peters, J. C. Relating N-H Bond Strengths to the Overpotential for Catalytic Nitrogen Fixation *Eur. J. Inorg. Chem.* **2020**, *2020*, 1353-1357. https://doi.org/10.1002/ejic.202000232
- (14) Chalkley, M. J.; Drover, M. W.; Peters, J. C. Catalytic N_2 -to- NH_3 (or $-N_2H_4$) Conversion by Well-Defined Molecular Coordination Complexes *Chem. Rev.* **2020**, *120*, 5582-5636.
- https://doi.org/10.1021/acs.chemrev.9b00638
- (15) MacFarlane, D. R.; Cherepanov, P. V.; Choi, J.; Suryanto, B. H. R.; Hodgetts, R. Y.; Bakker, J. M.; Ferrero Vallana, F. M.; Simonov, A. N. A Roadmap to the Ammonia Economy *Joule* **2020**, *4*, 1186-1205. https://www.sciencedirect.com/science/article/pii/S2542435120301732
- (16) Forrest, S. J. K.; Schluschaß, B.; Yuzik-Klimova, E. Y.; Schneider, S. Nitrogen Fixation via Splitting into Nitrido Complexes *Chem. Rev.* **2021**, *121*, 6522-6587. https://doi.org/10.1021/acs.chemrev.0c00958
- (17) Merakeb, L.; Robert, M. Advances in molecular electrochemical activation of dinitrogen *Current Opinion in Electrochemistry* **2021**, *29*, 100834. https://www.sciencedirect.com/science/article/pii/S2451910321001484
- (18) Yandulov, D. V.; Schrock, R. R. Catalytic Reduction of Dinitrogen to Ammonia at a Single Molybdenum Center *Science* **2003**, *301*, 76-78. http://www.sciencemag.org/content/301/5629/76
- (19) Arashiba, K.; Miyake, Y.; Nishibayashi, Y. A molybdenum complex bearing PNP-type pincer ligands leads to the catalytic reduction of dinitrogen into ammonia *Nat. Chem.* **2011**, *3*, 120-125. http://dx.doi.org/10.1038/nchem.906 (20) Tanabe, Y.; Nishibayashi, Y. Developing more sustainable processes for ammonia synthesis *Coord. Chem. Rev.*
- **2013**, *257*, 2551-2564. https://doi.org/10.1016/j.ccr.2013.02.010
- (21) Kuriyama, S.; Arashiba, K.; Nakajima, K.; Tanaka, H.; Kamaru, N.; Yoshizawa, K.; Nishibayashi, Y. Catalytic formation of ammonia from molecular dinitrogen by use of dinitrogen-bridged dimolybdenum-dinitrogen

- complexes bearing PNP-pincer ligands: Remarkable effect of substituent at PNP-pincer ligand *J. Am. Chem. Soc.* **2014**, *136*, 9719-9731. http://dx.doi.org/10.1021/ja5044243
- (22) Tanaka, H.; Arashiba, K.; Kuriyama, S.; Sasada, A.; Nakajima, K.; Yoshizawa, K.; Nishibayashi, Y. Unique behaviour of dinitrogen-bridged dimolybdenum complexes bearing pincer ligand towards catalytic formation of ammonia *Nat. Commun.* **2014**, *5*, 3737. http://dx.doi.org/10.1038/ncomms4737
- (23) Arashiba, K.; Kinoshita, E.; Kuriyama, S.; Eizawa, A.; Nakajima, K.; Tanaka, H.; Yoshizawa, K.; Nishibayashi, Y. Catalytic Reduction of Dinitrogen to Ammonia by Use of Molybdenum–Nitride Complexes Bearing a Tridentate Triphosphine as Catalysts *J. Am. Chem. Soc.* **2015**, *137*, 5666-5669. http://pubs.acs.org/doi/abs/10.1021/jacs.5b02579
- (24) Nishibayashi, Y. Recent Progress in Transition-Metal-Catalyzed Reduction of Molecular Dinitrogen under Ambient Reaction Conditions *Inorg. Chem.* **2015**, *54*, 9234-9247. https://doi.org/10.1021/acs.inorgchem.5b00881 (25) Tanaka, H.; Nishibayashi, Y.; Yoshizawa, K. Interplay between Theory and Experiment for Ammonia Synthesis Catalyzed by Transition Metal Complexes *Acc. Chem. Res.* **2016**, *49*, 987-995. http://dx.doi.org/10.1021/acs.accounts.6b00033
- (26) Eizawa, A.; Arashiba, K.; Tanaka, H.; Kuriyama, S.; Matsuo, Y.; Nakajima, K.; Yoshizawa, K.; Nishibayashi, Y. Remarkable catalytic activity of dinitrogen-bridged dimolybdenum complexes bearing NHC-based PCP-pincer ligands toward nitrogen fixation *Nat. Commun.* **2017**, *8*, 14874. http://www.ncbi.nlm.nih.gov/pmc/articles/PMC5382288/
- (27) Arashiba, K.; Eizawa, A.; Tanaka, H.; Nakajima, K.; Yoshizawa, K.; Nishibayashi, Y. Catalytic Nitrogen Fixation via Direct Cleavage of Nitrogen—Nitrogen Triple Bond of Molecular Dinitrogen under Ambient Reaction Conditions *Bull. Chem. Soc. Jpn.* **2017**, *90*, 1111-1118. https://doi.org/10.1246/bcsj.20170197
- (28) Ashida, Y.; Arashiba, K.; Nakajima, K.; Nishibayashi, Y. Molybdenum-catalysed ammonia production with samarium diiodide and alcohols or water *Nature* **2019**, *568*, 536-540. https://doi.org/10.1038/s41586-019-1134-2 (29) Itabashi, T.; Mori, I.; Arashiba, K.; Eizawa, A.; Nakajima, K.; Nishibayashi, Y. Effect of substituents on molybdenum triiodide complexes bearing PNP-type pincer ligands toward catalytic nitrogen fixation *Dalton Trans*. **2019**, *48*, 3182-3186. http://dx.doi.org/10.1039/C8DT04975K
- (30) Ashida, Y.; Nishibayashi, Y. Catalytic conversion of nitrogen molecule into ammonia using molybdenum complexes under ambient reaction conditions *Chem. Commun.* **2021**, *57*, 1176-1189.
- (31) Tanabe, Y.; Nishibayashi, Y. Comprehensive insights into synthetic nitrogen fixation assisted by molecular catalysts under ambient or mild conditions *Chem. Soc. Rev.* **2021**, *50*, 5201-5242. http://dx.doi.org/10.1039/D0CS01341B
- (32) Tanabe, Y.; Nishibayashi, Y. Recent advances in catalytic nitrogen fixation using transition metal-dinitrogen complexes under mild reaction conditions *Coord. Chem. Rev.* **2022**, *472*, 214783. https://doi.org/10.1016/j.ccr.2022.214783
- (33) Ashida, Y.; Mizushima, T.; Arashiba, K.; Egi, A.; Tanaka, H.; Yoshizawa, K.; Nishibayashi, Y. Catalytic production of ammonia from dinitrogen employing molybdenum complexes bearing N-heterocyclic carbene-based PCP-type pincer ligands *Nature Synthesis* **2023**, *2*, 635-644. https://doi.org/10.1038/s44160-023-00292-9
- (34) Mitsumoto, T.; Ashida, Y.; Arashiba, K.; Kuriyama, S.; Egi, A.; Tanaka, H.; Yoshizawa, K.; Nishibayashi, Y. Catalytic Activity of Molybdenum Complexes Bearing PNP-Type Pincer Ligand toward Ammonia Formation *Angew. Chem., Intl. Ed.* **2023**, *n/a*, e202306631. https://doi.org/10.1002/anie.202306631
- (35) Hebden, T. J.; Schrock, R. R.; Takase, M. K.; Muller, P. Cleavage of dinitrogen to yield a (t-BuPOCOP)molybdenum(IV) nitride *Chem. Commun.* **2012**, *48*, 1851-1853. http://dx.doi.org/10.1039/C2CC17634C (36) Klopsch, I.; Finger, M.; Würtele, C.; Milde, B.; Werz, D. B.; Schneider, S. Dinitrogen Splitting and Functionalization in the Coordination Sphere of Rhenium *J. Am. Chem. Soc.* **2014**, *136*, 6881-6883. http://dx.doi.org/10.1021/ja502759d
- (37) Liao, Q.; Cavaillé, A.; Saffon-Merceron, N.; Mézailles, N. Direct Synthesis of Silylamine from N2 and a Silane: Mediated by a Tridentate Phosphine Molybdenum Fragment *Angew. Chem., Intl. Ed.* **2016**, *55*, 11212-11216. http://dx.doi.org/10.1002/anie.201604812
- (38) Silantyev, G. A.; Förster, M.; Schluschaß, B.; Abbenseth, J.; Würtele, C.; Volkmann, C.; Holthausen, M. C.; Schneider, S. Dinitrogen Splitting Coupled to Protonation *Angew. Chem., Intl. Ed.* **2017**, *56*, 5872-5876. http://dx.doi.org/10.1002/anie.201701504
- (39) Lindley, B. M.; van Alten, R. S.; Finger, M.; Schendzielorz, F.; Würtele, C.; Miller, A. J. M.; Siewert, I.; Schneider, S. Mechanism of Chemical and Electrochemical N₂ Splitting by a Rhenium Pincer Complex *J. Am. Chem. Soc.* **2018**, 140, 7922-7935. https://doi.org/10.1021/jacs.8b03755

- (40) Espada, M. F.; Bennaamane, S.; Liao, Q.; Saffon-Merceron, N.; Massou, S.; Clot, E.; Nebra, N.; Fustier-Boutignon, M.; Mezailles, N. Room-Temperature Functionalization of N₂ to Borylamine at a Molybdenum Complex Angew. Chem., Intl. Ed. 2018, 57, 12865-12868. https://doi.org/10.1002/anie.201805915
- (41) Eizawa, A.; Arashiba, K.; Egi, A.; Tanaka, H.; Nakajima, K.; Yoshizawa, K.; Nishibayashi, Y. Catalytic Reactivity of Molybdenum–Trihalide Complexes Bearing PCP-Type Pincer Ligands Chem. Asian J. 2019, 14, 2091-2096. https://doi.org/10.1002/asia.201900496
- (42) Ashida, Y.; Kondo, S.; Arashiba, K.; Kikuchi, T.; Nakajima, K.; Kakimoto, S.; Nishibayashi, Y. A Practical Synthesis of Ammonia from Nitrogen Gas, Samarium Diiodide and Water Catalyzed by a Molybdenum-PCP Pincer Complex Synthesis 2019, 51, 3792-3795.
- (43) Egi, A.; Tanaka, H.; Konomi, A.; Nishibayashi, Y.; Yoshizawa, K. Nitrogen Fixation Catalyzed by Dinitrogen-Bridged Dimolybdenum Complexes Bearing PCP- and PNP-Type Pincer Ligands: A Shortcut Pathway Deduced from Free Energy Profiles Eur. J. Inorg. Chem. 2020, 2020, 1490-1498.
- (44) Song, J. Y.; Liao, Q.; Hong, X.; Jin, L.; Mezailles, N. Conversion of Dinitrogen into Nitrile: Cross-Metathesis of N₂-Derived Molybdenum Nitride with Alkynes Angew. Chem., Intl. Ed. 2021, 60, 12242-12247. https://doi.org/10.1002/anie.202015183
- (45) Garrido-Barros, P.; Derosa, J.; Chalkley, M. J.; Peters, J. C. Tandem electrocatalytic N₂ fixation via protoncoupled electron transfer Nature 2022, 609, 71-76. https://doi.org/10.1038/s41586-022-05011-6
- (46) Ashida, Y.; Onozuka, Y.; Arashiba, K.; Konomi, A.; Tanaka, H.; Kuriyama, S.; Yamazaki, Y.; Yoshizawa, K.; Nishibayashi, Y. Catalytic nitrogen fixation using visible light energy Nat. Commun. 2022, 13, 7263. https://doi.org/10.1038/s41467-022-34984-1
- (47) Itabashi, T.; Arashiba, K.; Egi, A.; Tanaka, H.; Sugiyama, K.; Suginome, S.; Kuriyama, S.; Yoshizawa, K.; Nishibayashi, Y. Direct synthesis of cyanate anion from dinitrogen catalysed by molybdenum complexes bearing pincer-type ligand Nat. Commun. 2022, 13, 6161.
- (48) Itabashi, T.; Arashiba, K.; Kuriyama, S.; Nishibayashi, Y. Reactivity of molybdenum-nitride complex bearing pyridine-based PNP-type pincer ligand toward carbon-centered electrophiles Dalton Trans. 2022, 51, 1946-1954. https://doi.org/10.1039/d1dt03952k
- (49) Merakeb, L.; Bennaamane, S.; De Freitas, J.; Clot, E.; Mezailles, N.; Robert, M. Molecular Electrochemical Reductive Splitting of Dinitrogen with a Molybdenum Complex Angew. Chem., Intl. Ed. 2022, 61, e202209899. https://doi.org/10.1002/anie.202209899
- (50) Coffinet, A.; Specklin, D.; Le De, Q.; Bennaamane, S.; Munoz, L.; Vendier, L.; Clot, E.; Mezailles, N.; Simonneau, A. Assessing Combinations of B(C₆F₅)₃ and N₂-Derived Molybdenum Nitrido Complexes for Heterolytic Bond Activation Chem. - Eur. J. 2023, 29, e202203774.
- (51) Ibrahim, A. F.; Garrido-Barros, P.; Peters, J. C. Electrocatalytic Nitrogen Reduction on a Molybdenum Complex Bearing a PNP Pincer Ligand ACS Catal. 2023, 13, 72-78. https://doi.org/10.1021/acscatal.2c04769
- (52) Ostermann, N.; Rotthowe, N.; Stückl, A. C.; Siewert, I. (Electro)chemical N₂ Splitting by a Molybdenum Complex with an Anionic PNP Pincer-Type Ligand ACS Organic & Inorganic Au 2024. https://doi.org/10.1021/acsorginorgau.3c00056
- (53) Schrock, R. R. Catalytic reduction of dinitrogen to ammonia at a single molybdenum center Acc. Chem. Res. **2005**, 38, 955-962. https://doi.org/10.1021/ar0501121
- (54) Zhou, X.; Malakar, S.; Zhou, T.; Murugesan, S.; Huang, C.; Emge, T. J.; Krogh-Jespersen, K.; Goldman, A. S. Catalytic Alkane Transfer Dehydrogenation by PSP-Pincer-Ligated Ruthenium. Deactivation of an Extremely Reactive Fragment by Formation of Allyl Hydride Complexes ACS Catal. 2019, 9, 4072-4083. https://doi.org/10.1021/acscatal.8b05172
- (55) Liao, Q.; Saffon-Merceron, N.; Mezailles, N. N2 Reduction into Silylamine at Tridentate Phosphine/Mo Center: Catalysis and Mechanistic Study ACS Catal. 2015, 5, 6902-6906. https://doi.org/10.1021/acscatal.5b01626
- (56) Kuriyama, S.; Arashiba, K.; Nakajima, K.; Tanaka, H.; Yoshizawa, K.; Nishibayashi, Y. Azaferrocene-Based PNP-Type Pincer Ligand: Synthesis of Molybdenum, Chromium, and Iron Complexes and Reactivity toward Nitrogen Fixation Eur. J. Inorg. Chem. 2016, 2016, 4856-4861. https://doi.org/10.1002/ejic.201601051
- (57) Bruch, Q. J.; Malakar, S.; Goldman, A. S.; Miller, A. J. M. Mechanisms of Electrochemical N₂ Splitting by a Molybdenum Pincer Complex Inorg. Chem. 2022, 61, 2307–2318. https://doi.org/10.1021/acs.inorgchem.1c03698
- (58) Hasanayn, F.; Holland, P. L.; Goldman, A. S.; Miller, A. J. M. Lewis Structures and the Bonding Classification of End-on Bridging Dinitrogen Transition Metal Complexes J. Am. Chem. Soc. 2023.

https://doi.org/10.1021/jacs.2c12243

(59) In marked contrast with the reaction conducted in the presence of added I⁻, in the absence of added I⁻ a complex mixture of products was observed by ³¹P and ¹H NMR spectroscopy, including the "over-reduced" N₂bridged Mo(0) complex (2) as well as some remaining Mo(III) 1-Cl₃.

- (60) Katayama, A.; Ohta, T.; Wasada-Tsutsui, Y.; Inomata, T.; Ozawa, T.; Ogura, T.; Masuda, H. Dinitrogen-Molybdenum Complex Induces Dinitrogen Cleavage by One-Electron Oxidation *Angew. Chem., Intl. Ed.* **2019**, *58*, 11279-11284. https://doi.org/10.1002/anie.201905299
- (61) Zhang, G.; Liu, T.; Song, J.; Quan, Y.; Jin, L.; Si, M.; Liao, Q. N₂ Cleavage on d⁴/d⁴ Molybdenum Centers and Its Further Conversion into Iminophosphorane under Mild Conditions *J. Am. Chem. Soc.* **2022**, *144*, 2444-2449. https://doi.org/10.1021/jacs.1c11134
- (62) Kani, Y.; Takayama, T.; Sekine, T.; Kudo, H. Crystal structures of nitridotechnetium(V) complexes of amine oximes differing in carbon chain lengths *J. Chem. Soc., Dalton Trans.* **1999**, 209-214. http://dx.doi.org/10.1039/A806245E
- (63) Weber, J. E.; Hasanayn, F.; Fataftah, M.; Mercado, B. Q.; Crabtree, R. H.; Holland, P. L. Electronic and Spin-State Effects on Dinitrogen Splitting to Nitrides in a Rhenium Pincer System *Inorg. Chem.* **2021**, *60*, 6115-6124. https://doi.org/10.1021/acs.inorgchem.0c03778
- (64) Laplaza, C. E.; Johnson, M. J. A.; Peters, J. C.; Odom, A. L.; Kim, E.; Cummins, C. C.; George, G. N.; Pickering, I. J. Dinitrogen Cleavage by Three-Coordinate Molybdenum(III) Complexes: Mechanistic and Structural Data *J. Am. Chem. Soc.* **1996**, *118*, 8623-8638. http://pubs.acs.org/doi/abs/10.1021/ja960574x
- (65) Klopsch, I.; Yuzik-Klimova, E. Y.; Schneider, S. In *Nitrogen Fixation*; Nishibayashi, Y., Ed.; Springer International Publishing: Cham, 2017, p 71-112.
- (66) Lindley, B.; Miller, A. J.; Schneider, S.; American Chemical Society: 2020, p SWRM-RMRM-172.
- (67) van Alten, R. S.; Waetjen, F.; Demeshko, S.; Miller, A. J. M.; Wuertele, C.; Siewert, I.; Schneider, S.
- (Electro-)chemical Splitting of Dinitrogen with a Rhenium Pincer Complex *Eur. J. Inorg. Chem.* **2020**, *2020*, 1402-1410. https://doi.org/10.1002/ejic.201901278
- (68) Brookhart, M.; Grant, B.; Volpe, A. F. $[(3,5-(CF_3)_2C_6H_3)_4B]^-[H(OEt_2)_2]^+$: a convenient reagent for generation and stabilization of cationic, highly electrophilic organometallic complexes *Organometallics* **1992**, *11*, 3920-3922. http://dx.doi.org/10.1021/om00059a071
- (69) Yandulov, D. V.; Schrock, R. R.; Rheingold, A. L.; Ceccarelli, C.; Davis, W. M. Synthesis and reactions of molybdenum triamidoamine complexes containing hexaisopropylterphenyl substituents *Inorg. Chem.* **2003**, *42*, 796-813. https://doi.org/10.1021/ic0205051
- (70) For a closely related example of an oxidative reaction of a pincer-Re complex with ammonia to yield a nitride complex, see: Connor, G. P.; Delony, D.; Weber, J. E.; Mercado, B. Q.; Curley, J. B.; Schneider, S.; Mayer, J. M.; Holland, P. L., Facile conversion of ammonia to a nitride in a rhenium system that cleaves dinitrogen *Chem. Sci.* **2022**, *13*, 4010-4018.
- (71) Frisch, M. J.; Trucks, G. W.; Schlegel, H. B.; Scuseria, G. E.; Robb, M. A.; Cheeseman, J. R.; Scalmani, G.; V. Barone; Petersson, G. A.; Nakatsuji, H.; X. Li; Caricato, M.; Marenich, A. V.; Bloino, J.; Janesko, B. G.; Gomperts, R.; Mennucci, B.; Hratchian, H. P.; Ortiz, J. V.; Izmaylov, A. F.; Sonnenberg, J. L.; Williams-Young, D.; Ding, F.; Lipparini, F.; Egidi, F.; Goings, J.; Peng, B.; Petrone, A.; Henderson, T.; Ranasinghe, D.; Zakrzewski, V. G.; Gao, J.; Rega, N.; Zheng, G.; Liang, W.; M. Hada; Ehara, M.; Toyota, K.; Fukuda, R.; Hasegawa, J.; Ishida, M.; Nakajima, T.; Honda, Y.; Kitao, O.; Nakai, H.; Vreven, T.; Throssell, K.; Montgomery, J. A.; Peralta, J. E.; Ogliaro, F.; Bearpark, M. J.; Heyd, J. J.; Brothers, E. N.; Kudin, K. N.; Staroverov, V. N.; Keith, T. A.; Kobayashi, R.; Normand, J.; Raghavachari, K.; Rendell, A. P.; J. C. Burant; Iyengar, S. S.; Tomasi, J.; Cossi, M.; Millam, J. M.; Klene, M.; Adamo, C.; Cammi, R.; Ochterski, J. W.; Martin, R. L.; Morokuma, K.; Farkas, O.; Foresman, J. B.; Fox, D. J. Gaussian 16, Revision A.03, Gaussian, Inc., Wallingford, CT, 2016.
- (72) Yu, H. S.; He, X.; Li, S. L.; Truhlar, D. G. MN15: A Kohn–Sham global-hybrid exchange–correlation density functional with broad accuracy for multi-reference and single-reference systems and noncovalent interactions *Chem. Sci.* **2016**, *7*, 5032-5051. http://dx.doi.org/10.1039/C6SC00705H
- (73) Francl, M. M.; Pietro, W. J.; Hehre, W. J.; Binkley, J. S.; Gordon, M. S.; DeFrees, D. J.; Pople, J. A. Self-consistent molecular orbital methods XXIII A polarization-type basis set for second-row elements *J. Chem. Phys.* **1982**, *77*, 3654-3665. https://doi.org/10.1063/1.444267
- (74) Gordon, M. S.; Binkley, J. S.; Pople, J. A.; Pietro, W. J.; Hehre, W. J. Self-consistent molecular-orbital methods. 22. Small split-valence basis sets for second-row elements *J. Am. Chem. Soc.* **1982**, *104*, 2797-2803. https://doi.org/10.1021/ja00374a017
- (75) Andrae, D.; Haeussermann, U.; Dolg, M.; Stoll, H.; Preuss, H. Energy-adjusted ab initio pseudopotentials for the second and third row transition elements *Theor. Chim. Acta* **1990**, *77*, 123-141. https://doi.org/10.1007/BF01114537
- (76) Peterson, K. A.; Figgen, D.; Goll, E.; Stoll, H.; Dolg, M. Systematically convergent basis sets with relativistic pseudopotentials. II. Small-core pseudopotentials and correlation consistent basis sets for the post-d group 16–18 elements *J. Chem. Phys.* **2003**, *119*, 11113-11123. https://doi.org/10.1063/1.1622924

- (77) Rappoport, D.; Furche, F. Property-optimized Gaussian basis sets for molecular response calculations *J. Chem. Phys.* **2010**, *133*, 134105. https://doi.org/10.1063/1.3484283
- (78) Weigend, F.; Ahlrichs, R. Balanced basis sets of split valence, triple zeta valence and quadruple zeta valence quality for H to Rn: Design and assessment of accuracy *Phys. Chem. Chem. Phys.* **2005**, *7*, 3297-3305. http://dx.doi.org/10.1039/B508541A
- (79) Weigend, F.; Furche, F.; Ahlrichs, R. Gaussian basis sets of quadruple zeta valence quality for atoms H–Kr *J. Chem. Phys.* **2003**, *119*, 12753-12762. https://doi.org/10.1063/1.1627293
- (80) Marenich, A. V.; Cramer, C. J.; Truhlar, D. G. Universal Solvation Model Based on Solute Electron Density and on a Continuum Model of the Solvent Defined by the Bulk Dielectric Constant and Atomic Surface Tensions *J. Phys. Chem. B* **2009**, *113*, 6378-6396. https://doi.org/10.1021/jp810292n
- (81) Bezier, D.; Guan, C.; Krogh-Jespersen, K.; Goldman, A. S.; Brookhart, M. Experimental and Computational Study of Alkane Dehydrogenation Catalyzed by a Carbazolide-based Rhodium PNP Pincer Complex *Chem. Sci.* **2016**, 7, 2579-2586. http://pubs.rsc.org/en/content/articlepdf/2016/sc/c5sc04794c
- (82) Auer, B.; Fernandez, L. E.; Hammes-Schiffer, S. Theoretical Analysis of Proton Relays in Electrochemical Proton-Coupled Electron Transfer *J. Am. Chem. Soc.* **2011**, *133*, 8282-8292. https://doi.org/10.1021/ja201560v
- (83) Arashiba, K.; Tanaka, H.; Yoshizawa, K.; Nishibayashi, Y. Cycling between Molybdenum-Dinitrogen and -Nitride Complexes to Support the Reaction Pathway for Catalytic Formation of Ammonia from Dinitrogen *Chem.-Eur. J.* **2020**, *26*, 13383-13389. https://doi.org/10.1002/chem.202002200
- (84) Wang, T.; Abild-Pedersen, F. Achieving industrial ammonia synthesis rates at near-ambient conditions through modified scaling relations on a confined dual site *Proc. Natl. Acad. Sci.* **2021**, *118*, e2106527118. https://doi.org/10.1073/pnas.2106527118
- (85) van der Ham, C. J. M.; Koper, M. T. M.; Hetterscheid, D. G. H. Challenges in reduction of dinitrogen by proton and electron transfer *Chem. Soc. Rev.* **2014**, *43*, 5183-5191. http://dx.doi.org/10.1039/C4CS00085D
- (86) Wang, S.; Ichihara, F.; Pang, H.; Chen, H.; Ye, J. Nitrogen Fixation Reaction Derived from Nanostructured Catalytic Materials *Advanced Functional Materials* **2018**, *28*, 1803309. https://doi.org/10.1002/adfm.201803309 (87) Shao, M.; Shao, Y.; Chen, W.; Ao, K. L.; Tong, R.; Zhu, Q.; Chan, I. N.; Ip, W. F.; Shi, X.; Pan, H. Efficient nitrogen fixation to ammonia on MXenes *Phys. Chem. Chem. Phys.* **2018**, *20*, 14504-14512.

http://dx.doi.org/10.1039/C8CP01396A

- (88) Liu, Y.; Su, Y.; Quan, X.; Fan, X.; Chen, S.; Yu, H.; Zhao, H.; Zhao, J. Facile Ammonia Synthesis from Electrocatalytic N₂ Reduction under Ambient Conditions on N-Doped Porous Carbon *ACS Catal.* **2018**, *8*, 1186-1191. https://doi.org/10.1021/acscatal.7b02165
- (89) Chatt, J.; Pearman, A. J.; Richards, R. L. The reduction of mono-coordinated molecular nitrogen to ammonia in a protic environment *Nature* **1975**, *253*, 39-40. http://dx.doi.org/10.1038/253039b0
- (90) Chatt, J.; Dilworth, J. R.; Richards, R. L. Recent advances in the chemistry of nitrogen fixation *Chem. Rev.* **1978**, 78, 589-625. http://dx.doi.org/10.1021/cr60316a001
- (91) Schrock, R. R. Catalytic reduction of dinitrogen under mild conditions *Chem. Commun.* **2003**, 2389-2391. http://dx.doi.org/10.1039/B307784P
- (92) Yandulov, D. V.; Schrock, R. R. Studies relevant to catalytic reduction of dinitrogen to ammonia by molybdenum triamidoamine complexes *Inorg. Chem.* **2005**, *44*, 1103-1117. http://dx.doi.org/10.1021/ic040095w (93) Schrock, R. R. Catalytic reduction of dinitrogen to ammonia by molybdenum: Theory versus experiment *Angew. Chem., Intl. Ed.* **2008**, *47*, 5512-5522.
- (94) Wickramasinghe, L. A.; Ogawa, T.; Schrock, R. R.; Müller, P. Reduction of Dinitrogen to Ammonia Catalyzed by Molybdenum Diamido Complexes *J. Am. Chem. Soc.* **2017**, *139*, 9132-9135. https://doi.org/10.1021/jacs.7b04800
- (95) Anderson, J. S.; Rittle, J.; Peters, J. C. Catalytic conversion of nitrogen to ammonia by an iron model complex *Nature* **2013**, *501*, 84-87. http://dx.doi.org/10.1038/nature12435
- (96) Creutz, S. E.; Peters, J. C. Catalytic reduction of N_2 to NH_3 by an Fe- N_2 complex featuring a C-atom anchor *J. Am. Chem. Soc.* **2014**, *136*, 1105-1115. http://dx.doi.org/10.1021/ja4114962
- (97) Agarwal, R. G.; Coste, S. C.; Groff, B. D.; Heuer, A. M.; Noh, H.; Parada, G. A.; Wise, C. F.; Nichols, E. M.; Warren, J. J.; Mayer, J. M. Free Energies of Proton-Coupled Electron Transfer Reagents and Their Applications *Chem. Rev.* **2022**, *122*, 1-49. https://doi.org/10.1021/acs.chemrev.1c00521
- (98) Jones, L.; Lin, L. A theoretical study on the isomers of the B5TB heteroacene for improved semiconductor properties in organic electronics *Comput. Theor. Chem.* **2017**, *1115*, 22-29. https://doi.org/10.1016/j.comptc.2017.05.039
- (99) Buchanan, E. A.; Michl, J. Optimal arrangements of 1,3-diphenylisobenzofuran molecule pairs for fast singlet fission *Photochem. Photobiol. Sci.* **2019**, *18*, 2112-2124. https://doi.org/10.1039/c9pp00283a